

# NAVAL POSTGRADUATE SCHOOL Monterey, California

AD-A225 400



DTIC  
ELECTE  
AUG 17 1990  
S B D  
P

## THESIS

APPLICATION OF H<sub>L</sub> METHOD TO  
MODERN FIGHTER CONFIGURATION

by

Hsu, Ta-Chieh

December, 1989

Thesis Advisor:

Prof. D. J. Collins

Approved for public release; distribution is unlimited.

REPORT DOCUMENTATION PAGE			
1a REPORT SECURITY CLASSIFICATION Unclassified		1b RESTRICTIVE MARKINGS	
2a SECURITY CLASSIFICATION AUTHORITY		3 DISTRIBUTION/AVAILABILITY OF REPORT Approved for public release; distribution is unlimited.	
2b DECLASSIFICATION/DOWNGRADING SCHEDULE			
4. PERFORMING ORGANIZATION REPORT NUMBER(S)		5 MONITORING ORGANIZATION REPORT NUMBER(S)	
6a NAME OF PERFORMING ORGANIZATION Naval Postgraduate School	6b OFFICE SYMBOL (If applicable) 55	7a NAME OF MONITORING ORGANIZATION Naval Postgraduate School	
6c ADDRESS (City, State, and ZIP Code) Monterey, CA 93943-5000		7b ADDRESS (City, State, and ZIP Code) Monterey, CA 93943-5000	
8a NAME OF FUNDING/SPONSORING ORGANIZATION	8b OFFICE SYMBOL (If applicable)	9 PROCUREMENT INSTRUMENT IDENTIFICATION NUMBER	
8c ADDRESS (City, State, and ZIP Code)		10 SOURCE OF FUNDING NUMBERS	
		Program Element No	Project No
		Task No	Work Unit Accession Number
11. TITLE (Include Security Classification) Application of H <sup>∞</sup> Method to Modern Fighter Configuration <i>Inf...</i>			
12. PERSONAL AUTHOR(S) Hsu, Ta-Chieh			
13a TYPE OF REPORT Master's Thesis	13b TIME COVERED From To	14. DATE OF REPORT (year, month, day) 1989, December	15 PAGE COUNT 88
16. SUPPLEMENTARY NOTATION The views expressed in this thesis are those of the author and do not reflect the official policy or position of the Department of Defense or the U.S. Government.			
17. COSATI CODES		18 SUBJECT TERMS (continue on reverse if necessary and identify by block number)	
FIELD	GROUP	H <sup>∞</sup> Control Theory, Robust Control Systems, Sensitivity, Disturbance Attenuation, X-29 Controller Synthesis, Augmented Plant, Small Gain Problem	
19 ABSTRACT (continue on reverse if necessary and identify by block number) An optimal control theory, based on singular value loop shaping, is used to synthesize a controller for the statically unstable longitudinal dynamics of X-29 aircraft. Two design cases are studied: 2-input 2-output; and 3-input 3-output cases. The theory provides a direct, effective procedure for synthesizing control laws satisfying specified performance objectives and robustness specifications. The 2 I/O case has better performance, a better response and is more robust, than 3 I/O case. Discussion and comparison of results are given.			
20 DISTRIBUTION/AVAILABILITY OF ABSTRACT <input checked="" type="checkbox"/> UNCLASSIFIED/UNLIMITED <input checked="" type="checkbox"/> SAME AS REPORT <input type="checkbox"/> DTIC USERS		21 ABSTRACT SECURITY CLASSIFICATION Unclassified	
22a NAME OF RESPONSIBLE INDIVIDUAL Dr. D. J. Collins		22b TELEPHONE (Include Area code) (408) 646-2628	22c OFFICE SYMBOL 67Co

Approved for public release; distribution is unlimited.

**APPLICATION OF H<sub>∞</sub> METHOD TO MODERN FIGHTER CONFIGURATION**

by

**Hsu, Ta-Chieh**

**Captain, Republic of China on Taiwan Army  
B.S., Chung Cheng Institute of Technology, 1983**

**Submitted in partial fulfillment  
of the requirements for the degree of**

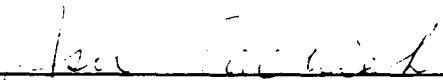
**MASTER OF SCIENCE IN ENGINEERING SCIENCE  
(MAJOR IN MECHANICAL ENGINEERING)**

from the

**NAVAL POSTGRADUATE SCHOOL**

**December 1989**

**Author:**

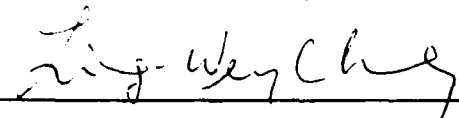
  
\_\_\_\_\_

**Hsu, Ta-Chieh**

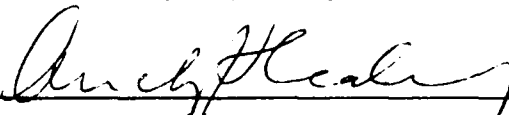
**Approved by:**

  
\_\_\_\_\_

**D. J. Collins, Thesis Advisor**

  
\_\_\_\_\_

**Liang-Wey Chang, Second Reader**

  
\_\_\_\_\_

**A. J. Healey, Chairman**

**Department of Mechanical Engineering**

## ABSTRACT

$H_{\infty}$  optimal control theory, based on singular value loop shaping, is used to synthesize a controller for the statically unstable longitudinal dynamics of X-29 aircraft. Two design cases are studied: 2-input 2-output; and 3-input 3-output cases.  $H_{\infty}$  theory provides a direct, effective procedure for synthesizing control laws satisfying specified performance objectives and robustness specifications. The 2 I/O case has better performance, a faster response and is more robust, than the 3 I/O case. Discussion and comparison of results are given.

## TABLE OF CONTENTS

I. INTRODUCTION .....	1
II. FEEDBACK PROPERTIES .....	3
A. RETURN DIFFERENCE MATRIX .....	3
B. SINGULAR VALUES AND MATRIX NORM .....	5
C. SENSITIVITY FUNCTION AND DISTURBANCE ATTENUATION	6
D. STABILITY AND STABILITY MARGIN .....	9
III. $H_2$ CONTROL DESIGN .....	10
A. CONTROL SYSTEM FORMULATION .....	11
B. $H_2$ OPTIMAL CONTROL PROBLEM .....	14
C. WEIGHTING MATRIX SELECTION .....	17
IV. $H_2$ CONTROLLER SYNTHESIS FOR X-29 FIGHTER .....	21
A. PLANT DESCRIPTION .....	21
B. DESIGN SPECIFICATIONS AND WEIGHTING FUNCTIONS .....	28
C. DESIGN PROCEDURE .....	30
1. 2-INPUT, 2-OUTPUT DESIGN CASE .....	30
2. 3-INPUT, 3-OUTPUT DESIGN CASE .....	43

V. CONCLUSIONS AND RECOMMENDATIONS . . . . . 53

    APPENDIX A . . . . . 54

    APPENDIX B . . . . . 68

    APPENDIX C . . . . . 69

    APPENDIX D . . . . . 71

    APPENDIX E . . . . . 75

    REFERENCES . . . . . 76

    INITIAL DISTRIBUTION LIST . . . . . 78

<b>Accession For</b>	
NTIS GRA&I	<input checked="" type="checkbox"/>
DTIC TAB	<input type="checkbox"/>
Unannounced	<input type="checkbox"/>
Justification	
By _____	
Distribution/	
Availability Codes	
Dist	Avail and/or Special
A-1	

## LIST OF FIGURES

Figure 2.1	Standard Feedback Control System . . . . .	4
Figure 2.2	Finite Dimensional Linear time Invariant System . . . . .	7
Figure 3.1	Standard $H_\infty$ Small Gain Problem . . . . .	10
Figure 3.2	Compensated System with Augmented Plant $P(s)$ . . . . .	11
Figure 3.3	Additive / Multiplicative uncertainty . . . . .	15
Figure 3.4	Singular Value Spec's on $S(s)$ and $T(s)$ . . . . .	19
Figure 3.5	$H_\infty$ Singular Value Loop Shaping Iterative Process . . . . .	20
Figure 4.1	FSW X-29 Fighter . . . . .	22
Figure 4.2	X-29 2-Input, 2-Output Open Loop Configuration . . . . .	24
Figure 4.3	X-29 3 I/O Open Loop Configuration . . . . .	25
Figure 4.4	Singular Value Plot of The Uncompensated Plant $G(s)$ . . . . .	27
Figure 4.5	Singular Value Plot of Weighting Functions . . . . .	29
Figure 4.6	Cost Function $T_{\gamma, \text{opt}}$ for $\gamma = 2.6$ . . . . .	31
Figure 4.7	Complementary Sensitivity Function $T(s)$ and $W_3^{-1}$ for $\gamma = 2.6$ . . . . .	32
Figure 4.8	Sensitivity Function $S(s)$ and $W_1^{-1}$ for $\gamma = 2.6$ . . . . .	32
Figure 4.9	X-29 Feedback Configuration . . . . .	34
Figure 4.10	Singular Value Plot of The Output Inverse-Return Difference Matrix for 2 I/O System . . . . .	36
Figure 4.11	Universal Gain and Phase Margin Curve . . . . .	36
Figure 4.12	Closed Loop Bode Plot of $\alpha$ and $q$ for 2 I/O System . . . . .	38
Figure 4.13	Step Response of $\alpha$ for 2 I/O System . . . . .	39

Figure 4.14	Step Response of $q$ for 2 I/O System . . . . .	39
Figure 4.15	Step Response of Canard Control Input $\delta_c$ and Flap Control Input $\delta_f$ . . . . .	40
Figure 4.16	Step Response of Strake Control Input $\delta_s$ . . . . .	41
Figure 4.17	Step Response of Canard Control Rate $\dot{\delta}_c$ . . . . .	41
Figure 4.18	Step Response of $\dot{\delta}_f$ and $\dot{\delta}_s$ . . . . .	42
Figure 4.19	Cost Function $T_{y,u_1}$ for $\gamma = 1.3$ . . . . .	44
Figure 4.20	Complementary Sensitivity $T(s)$ and Sensitivity $S(s)$ for $\gamma = 1.3$ . .	45
Figure 4.21	Output, Inverse Return Difference Matrix for 3 I/O System . . . . .	46
Figure 4.22	Closed Loop Bode Plots of $\alpha$ and $q$ for 3 I/O System . . . . .	47
Figure 4.23	Step Response of $\alpha$ and $q$ for 3 I/O System . . . . .	48
Figure 4.24	Step Response of $\delta_c$ and $\delta_f$ for 3 I/O System . . . . .	50
Figure 4.25	Step Response of $\delta_s$ for 3 I/O System . . . . .	51
Figure 4.26	Step Response of $\dot{\delta}_c$ for 3 I/O System . . . . .	51
Figure 4.27	Step Response of $\dot{\delta}_f$ and $\dot{\delta}_s$ for 3 I/O System . . . . .	52

## LIST OF TABLES

Table 4.1	Description of The Uncompensated X-29 state variables . . . . .	26
Table 4.2	Uncompensated X-29 open loop poles . . . . .	27
Table 4.3	Poles of The Reduced-Order Controller . . . . .	33
Table 4.4	Poles of The 2 I/O Closed Loop System . . . . .	35

## I. INTRODUCTION

The main task for control system designers is to synthesize a control law which maintains system response and error signals to within prespecified tolerances while at the same time ensure relatively high robustness. Some measures of system robustness commonly used are stability margins, sensitivity and disturbance attenuation. Thus, a robust system denotes a system with satisfied system performance, has large stability margins, good disturbance rejection and low sensitivity to parameter variations.

For the single-input single-output (SISO) systems, some techniques, i.e., root-locus method, Bode plot and Nyquist diagram, had been well developed to design and estimate system performance and robustness. Some of these classical methods can be generalized to multi-input multi-output (MIMO) systems, however, not all of them do. For instance, from a Nyquist diagram, one can not get a satisfactory notion of multivariable stability margins.

In the past decade, a lot of research on properties of multivariable feedback system has been accomplished. Singular value Bode plots of return difference and loop gain matrices have emerged as useful indicators of multivariable robustness [Refs. 1, 2, 3]. Among the techniques that have been recently developed,  $H_\infty$ , frequency-weighted LQG, and LQG loop transfer recovery optimal synthesis theories have made singular value loop shaping a routine matter [Ref. 5]. For a multivariable feedback control system, singular value loop shaping involves the manipulation of system loop gain over a specified frequency bandwidth to improve system performance and robustness.

$H_\infty$  theory provides a direct, reliable procedure for synthesizing a controller. While the frequency-weighted LQG optimal synthesis theory (or " $H_2$  theory") and LQG loop transfer recovery theory lead to somewhat less direct but highly effective iterative procedures for shaping singular value Bode plots to satisfy singular value loop shaping specification [Ref. 5].

The aim of this thesis is to present a controller design procedure, based on the  $H_\infty$  theory, for a reduced order, linearized longitudinal dynamics model of the X-29 aircraft analog backup mode. Some review about the properties of singular value, sensitivity reduction and return difference matrices will be given in Chapter II. In Chapter III,  $H_\infty$  theory and weighting matrix are introduced. Application of  $H_\infty$  theory to X-29 longitudinal dynamics model is made in Chapter IV. The design result is discussed in Chapter V.

## II. FEEDBACK PROPERTIES

For a control system, some properties such as impulse response matrix, transfer function matrix and other characterizations of the response to commands can be changed by prefiltering the command signal, rather than using feedback loop. But some properties, usually termed feedback properties, like stability, sensitivity and disturbance attenuation can be altered only through the feedback [Ref. 2]. Here, we focus on these feedback properties which also define the robustness of system.

### A. RETURN DIFFERENCE MATRIX

Consider the standard linear time-invariant multivariable feedback control system in Fig. 2.1. It consists of the interconnected plant (**G**), controller (**F**) and sensor (**H**) forced by commands (**r**), measurement noise (**n**), and plant disturbance (**d**). The prefilter (**P**) is an optional element used to achieve deliberate command shaping.

From this configuration, we get

plant

$$\mathbf{y}(s) = \mathbf{G}(s)\mathbf{u}(s) + \mathbf{d}(s) \quad (2.1)$$

controller

$$\mathbf{u}(s) = \mathbf{P}(s)\mathbf{r}(s) - \mathbf{F}(s)\mathbf{z}(s) \quad (2.2)$$

sensor

$$\mathbf{z}(s) = \mathbf{H}(s)(\mathbf{y}(s) + \mathbf{n}(s)) \quad (2.3)$$

where  $\mathbf{y}(s)$ ,  $\mathbf{d}(s)$ ,  $\mathbf{n}(s)$ ,  $\mathbf{u}(s)$ ,  $\mathbf{z}(s)$ ,  $\mathbf{r}(s)$  are vectors, and  $\mathbf{G}(s)$ ,  $\mathbf{F}(s)$ ,  $\mathbf{H}(s)$  are matrices.

For the feedback loop, define the transfer matrix

$$\mathbf{M}(s) \equiv \mathbf{F}(s)\mathbf{H}(s)$$

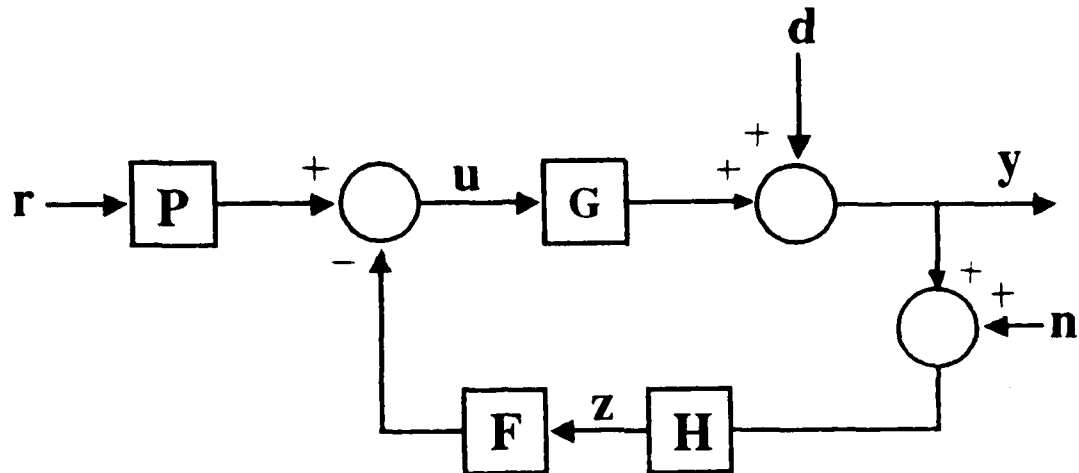


Figure 2.1 Standard Feedback Control System

and matrices

$$\mathbf{L}_2(s) \equiv \mathbf{G}(s)\mathbf{M}(s)$$

$$\mathbf{L}_1(s) \equiv \mathbf{M}(s)\mathbf{G}(s)$$

are called *return ratio* matrices [Ref. 2] at the  $y(s)$  node and the  $u(s)$  node, respectively.

And

$$\mathbf{I} + \mathbf{L}_2(s)$$

$$\mathbf{I} + \mathbf{L}_1(s)$$

are *return difference* matrices at  $y(s)$  node and  $u(s)$  node. Similarly, the  $y(s)$  node and  $u(s)$  node *inverse return difference* matrices are defined, respectively, as

$$\mathbf{I} + \mathbf{L}_2^{-1}$$

$$\mathbf{I} + \mathbf{L}_1^{-1}$$

Those terms introduced above are fundamental and important in the control system synthesis. Because for a SISO system, the phase and gain margins can be determined by the behavior of return difference as a function of frequency. And it turns out, as we will see later, the return difference matrix also provides a means of measuring robustness in a multivariable system.

## B. SINGULAR VALUES AND MATRIX NORM

In the design of a feedback loop, one needs to determine the "size" of matrix to estimate its properties. For a vector  $\mathbf{X}(x_1, x_2, x_3, \dots, x_n)$ , the size can be defined as the Euclidean norm

$$\|\mathbf{X}\| = \sqrt{x_1^2 + x_2^2 + x_3^2 + \dots + x_n^2}$$

For a matrix, a more general concept is needed. One way to describe the size of matrix  $\mathbf{A}$  is based on the largest singular value of  $\mathbf{A}$ , as

$$\bar{\sigma}(\mathbf{A}) = \max(\|\mathbf{AX}\| / \|\mathbf{X}\|)$$

where  $\|\cdot\|$  denotes Euclidean norms. The singular values  $\sigma_i$  of a rank  $n$  matrix  $\mathbf{A} \in \mathbb{C}^{m \times n}$  are defined as the non-negative square roots of the eigenvalues of  $\mathbf{A}^* \mathbf{A}$ , where  $\mathbf{A}^*$  is the transpose of the complex conjugate of  $\mathbf{A}$ . It is convenient to order them as follow

$$\sigma_1 \geq \sigma_2 \geq \sigma_3 \dots \geq \sigma_n$$

If rank  $r < n$ , then there are  $n - r$  zeros singular values, that is

$$\sigma_{r+1} = \sigma_{r+2} = \dots = \sigma_n = 0$$

One uses singular values rather than eigenvalues to describe matrix size since eigenvalues can be a very poor indicators of the "size" of matrix [Refs. 5, 14]. The singular value is also a good measure of the near-singularity of a matrix, i.e., how near the determinant of a matrix comes to being zero. The condition number, the ratio of the largest to the smallest singular value, provides information about sensitivity to perturbation, which also is an important indicator of robustness. Listed as follows are some useful properties of singular value :

- (1)  $\bar{\sigma}(A) = \max (\| AX \| / \| X \|)$
- (2)  $\underline{\sigma}(A) = \min (\| AX \| / \| X \|)$  (the least singular value of A)
- (3)  $\underline{\sigma}(A) \leq | \lambda_i(A) | \leq \bar{\sigma}(A)$  , where  $\lambda_i$  denotes the i-th eigenvalue of A
- (4) If  $A^{-1}$  exists,  $\underline{\sigma}(A) = 1 / \bar{\sigma}(A^{-1})$
- (5) If  $A^{-1}$  exists,  $\bar{\sigma}(A) = 1 / \underline{\sigma}(A^{-1})$
- (6)  $\bar{\sigma}(AB) \leq \bar{\sigma}(A) \bar{\sigma}(B)$
- (7)  $\sum_{i=1}^n \sigma_i^2 = \text{Trace} (A^*A)$  [Ref. 5]

In SISO system, it is customary to define sensitivity in terms of percentage variation in system output resulting from a given percentage change in the plant with the input held fixed. A similar way is used to develop the sensitivity function for a MIMO system.

### C. SENSITIVITY FUNCTION AND DISTURBANCE ATTENUATION

Consider a finite dimensional linear time invariant (FDLTI) system in Fig. 2.2, where  $r$ ,  $d$ , and  $n$  are command, disturbance, and measure noise respectively. If it is asymptotically stable, then we have input-output loop error and sensitivity relation as follows :

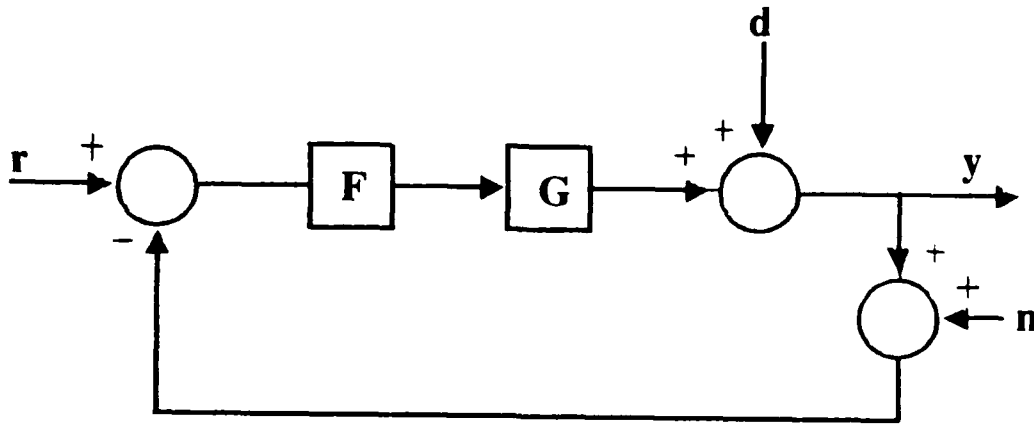


Figure 2.2 Finite Dimensional Linear time Invariant System

input-output

$$y = GF(I + GF)^{-1}(r - n) + (I + GF)^{-1}d \quad (2.4)$$

loop error

$$\begin{aligned} e &= r - y \\ &= (I + GF)^{-1}(r - d) + GF(I + GF)^{-1}n \end{aligned} \quad (2.5)$$

system sensitivity

$$\Delta H_{cl} = (I + G'F)^{-1}\Delta H_{ol} \quad (2.6)$$

where  $\Delta H_{cl}$  and  $\Delta H_{ol}$  represent the changes in the close-loop system and nominal open loop system caused by changes  $\Delta G$  in the plant  $G$ , i.e.,  $G' = G + \Delta G$  [Ref. 1].

Here, we define

$$S(s) \equiv (I + L(s))^{-1} = e/r \quad (2.7)$$

$$\mathbf{R}(s) \equiv \mathbf{F}(s)(\mathbf{I} + \mathbf{L}(s))^{-1} = \mathbf{u}/\mathbf{r} \quad (2.8)$$

$$\mathbf{T}(s) \equiv \mathbf{L}(s)(\mathbf{I} + \mathbf{L}(s))^{-1} = \mathbf{I} - \mathbf{S}(s) = \mathbf{y}/\mathbf{r} \quad (2.9)$$

where  $\mathbf{L}(s) = \mathbf{G}(s)\mathbf{F}(s)$  is the loop transfer function,  $\mathbf{S}(s)$  is known as the sensitivity function matrix,  $\mathbf{T}(s)$  is complementary sensitivity function. It can be seen that loop transfer function  $\mathbf{L}(s)$  determines the other three matrices. And, as will be seen, the singular value bode plots of these matrices play important role in the design of multivariable robust control system.

From Eq. (2.5), it is seen that the loop error " e " resulting from disturbance inputs can be made small by making the sensitivity matrix, or inverse of the return difference matrix  $(\mathbf{I} + \mathbf{GF})^{-1}$ , small. From Eq. (2.6) the system sensitivity to plant variations may be also reduced by decreasing the sensitivity function. One can decrease the size of the sensitivity function by making

$$\bar{\sigma}(\mathbf{S}(j\omega)) = \bar{\sigma}[(\mathbf{I} + \mathbf{L}(j\omega))^{-1}]$$

small, or (from singular value properties (5))

$$\underline{\sigma}(\mathbf{I} + \mathbf{L}(j\omega)) \quad (2.10)$$

large.

Note also

$$\underline{\sigma}(\mathbf{I} + \mathbf{L}(j\omega)) \approx \underline{\sigma}(\mathbf{L}(j\omega)) \quad \text{for } \underline{\sigma}(\mathbf{L}(j\omega)) \gg 1$$

This tells us that large loop gains or " tight " loops yield good performance. But one can not make loop gains arbitrarily high over arbitrarily large frequency. Since we can see, from Eq. (2.5), large  $\underline{\sigma}(\mathbf{L}(j\omega))$  over a large frequency range not only make errors due to  $\mathbf{r}$  and  $\mathbf{d}$  small, but make error due to  $\mathbf{n}$  large. Large gains can also lead to

instability. There are certain performance tradeoffs between command / disturbance error reduction and sensor noise error reduction and stability to be satisfied.

#### **D. STABILITY AND STABILITY MARGIN**

In SISO system, gain margin and phase margin are the stability margins that are commonly used. Both are conveniently expressed in terms of the magnitude of the return difference,  $I + L(j\omega)$ . In MIMO system, the return difference retains its importance, but the concept of gain margin and phase margin become problematic.

The stability of the system in Fig. 2.2 is directly related to the matrices  $S(s)$ ,  $R(s)$  and  $T(s)$ . To find the stability margin for the system is to determine a lower bound on the " size " of smallest perturbation to the plant that will destabilize the system. And the singular value Bode plot of  $S(s)$  and  $T(s)$  can be used as the measure of stability margins.

### III. $H_\infty$ CONTROL DESIGN

$H_\infty$  control theory provides a direct, reliable procedure for synthesizing a feedback controller designed to meet singular value loop shaping requirements. Its capability includes addressing the full range of stability margins, sensitivity, and robustness optimization and response-shaping problems that can be formulated within the singular value Bode plot framework. The standard configuration of an  $H_\infty$  problem is shown in Fig. 3.1. The design objective is to find a stabilizing controller  $F(s)$  for the augmented plant  $P(s)$  while keeping the robustness specifications satisfied.

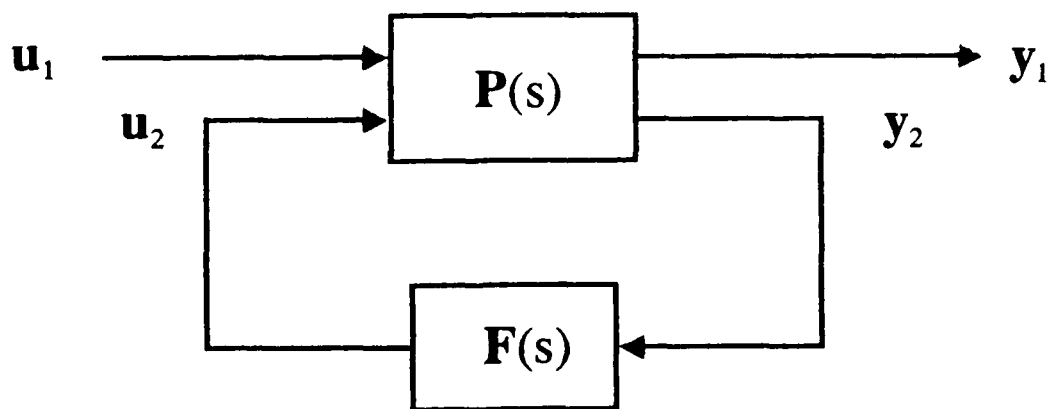


Figure 3.1 Standard  $H_\infty$  Small Gain Problem

The purpose of this chapter is to present a brief overview of  $H_\infty$  optimal theory and a control system design procedure based on this theory.

### A. CONTROL SYSTEM FORMULATION

As shown by Eq. (2.5), (2.6), and (2.10), the loop error due to disturbance and system sensitivity to plant variations can be reduced by suppressing the sensitivity function  $S(s)$ . (There is also some stability requirements desired in the robust system synthesizing.) These goals can be achieved by properly selecting the weighting functions in the design procedure.

Shown in Fig. 3.2, is the compensation configuration of system in Fig. 2.2, where  $P(s)$  is the augmented plant with weighting functions  $W_1$ ,  $W_2$  and  $W_3$ , which penalizing the error signal, control signal and output signal respectively.

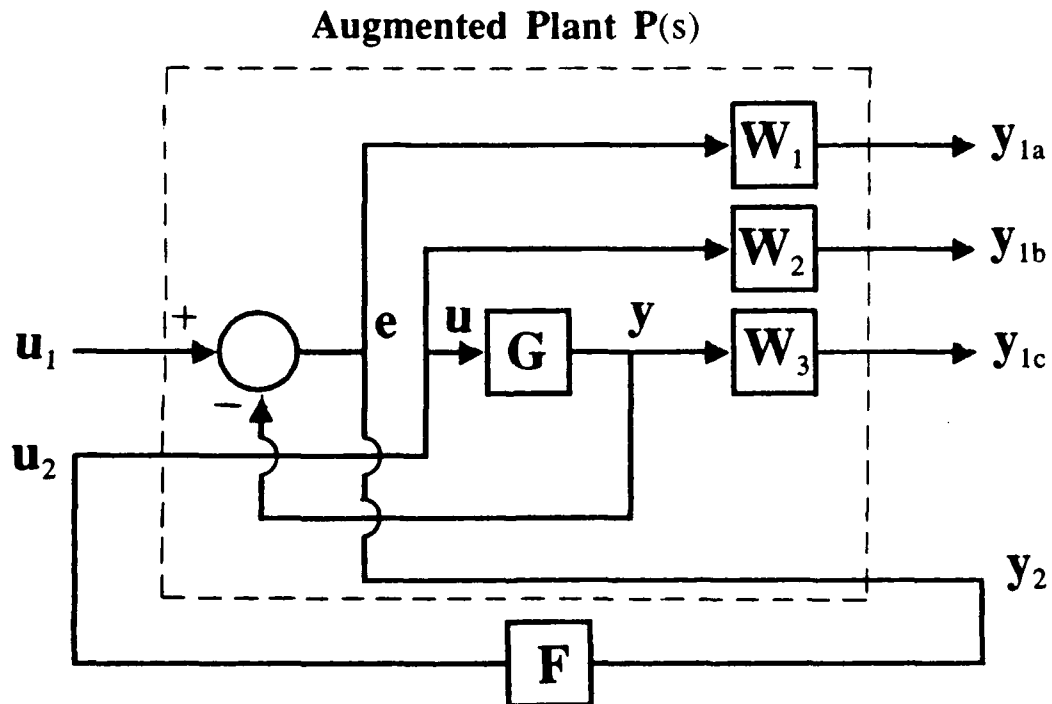


Figure 3.2 Compensated System with Augmented Plant  $P(s)$

From this Figure, we get

$$\begin{bmatrix} y_1 \\ y_2 \end{bmatrix} = \begin{bmatrix} y_{1a} \\ y_{1b} \\ y_{1c} \\ y_2 \end{bmatrix} = \begin{bmatrix} W_1 & -W_1 G \\ 0 & W_2 \\ 0 & W_3 G \\ I & -G \end{bmatrix} \begin{bmatrix} u_1 \\ u_2 \end{bmatrix}$$

Where the augmented plant with weighting functions is denoted as

$$P(s) = \begin{bmatrix} W_1 & -W_1 G \\ 0 & W_2 \\ 0 & W_3 G \\ I & -G \end{bmatrix}$$

A state space realization of  $P(s)$  is given by

$$P(s) = \begin{bmatrix} A & B_1 & B_2 \\ C_1 & D_{11} & D_{12} \\ C_2 & D_{21} & D_{22} \end{bmatrix} \quad (3.1)$$

$$= \begin{array}{c|cc|cc|cc} A_0 & 0 & 0 & 0 & 0 & B_0 \\ \hline -B_{w1}C_0 & A_{w1} & 0 & 0 & B_{w1} & -B_{w1}D_0 \\ 0 & 0 & A_{w2} & 0 & 0 & B_{w2} \\ B_{w3}C_0 & 0 & 0 & A_{w3} & 0 & B_{w3}D_0 \\ \hline -D_{w1}C_0 & C_{w1} & 0 & 0 & D_{w1} & -D_{w1}D_0 \\ 0 & 0 & C_{w2} & 0 & 0 & D_{w2} \\ D_{w3}C_0 & 0 & 0 & C_{w3} & 0 & D_{w3}D_0 \\ \hline -C_0 & 0 & 0 & 0 & I & -D_0 \end{array} \quad (3.2)$$

If the weighting transfer function is improper (i.e., has more zeros than poles), as can be the case for  $W_3$ , then no state space realization exists. The produce  $W_3G$  is in this case still proper and can be represented by a state space realization. Some calculations are need to compute the state space realization of the augmented plant.

From Fig. 3.1 one can define the transfer function  $T_{y_1u_1}$  as

$$y_1 = T_{y_1u_1} u_1 .$$

This transfer function can be expressed in terms of the weighting matrix and previous defined loop matrices, i.e.,

$$\begin{bmatrix} y_{1a} \\ y_{1b} \\ y_{1c} \end{bmatrix} = \begin{bmatrix} W_1S \\ W_2R \\ W_3T \end{bmatrix} u_1 .$$

And the close loop transfer function from input  $u_1$  to output  $y_1$  is denoted as

$$T_{y_1u_1} = \begin{bmatrix} W_1S \\ W_2R \\ W_3T \end{bmatrix} .$$

Where  $S$ ,  $R$ , and  $T$  are loop matrices defined in Eqs. (2.7), (2.8),(2.9).

The compensated system is said to be *internally stable* if the augmented  $A$  matrix of the compensated system is stable, i.e., when external input signal  $u_1$  equals to zero, the states of both  $P(s)$  and  $F(s)$  will go asymptotically to zero for any initial conditions. And the controller is said to be *stabilizing*.

## B. $H_\infty$ OPTIMAL CONTROL PROBLEM

The  $H_\infty$  optimal control problem is defined as the following small gain problem:

*For the given transfer function matrix  $P(s)$ , find a stabilizing controller  $F(s)$  such that the close loop transfer function matrix  $T_{y|u|}$  is internally stable and its infinity-norm is less than or equal to 1, i.e.,*

$$\| T_{y|u|} \|_\infty \leq 1. \quad (3.9)$$

Where the  $H_\infty$  - norm of matrix  $A$  is defined as

$$\| A \|_\infty \equiv \sup \bar{\sigma}(A(j\omega)). \quad (\text{sup : the least upper bound})$$

This problem is called a " small gain problem " because the closed loop gain is small (i.e., less than or equal to one). As mentioned before, the largest singular values of  $S(s)$  determine the plant disturbance attenuation, since  $S(s)$  is the same as the close loop transfer function from disturbance  $d$  to plant output  $y$  (Fig. 2.2). One may specify the system disturbance attenuation performance with the frequency-dependent weighting function  $W_1$ , that is

$$\bar{\sigma}(S(j\omega)) \leq | W_1^{-1}(j\omega) |$$

Now, consider the system in Fig. 3.4, where  $\Delta_A(s)$  and  $\Delta_M$  represent the additive plant perturbations and the multiplicative plant perturbations respectively. Defining the " size " of  $\Delta_A(j\omega)$  and  $\Delta_M(j\omega)$  as  $\bar{\sigma}(\Delta_A(j\omega))$  and  $\bar{\sigma}(\Delta_M(j\omega))$ , the stability theorems are obtained as follows:

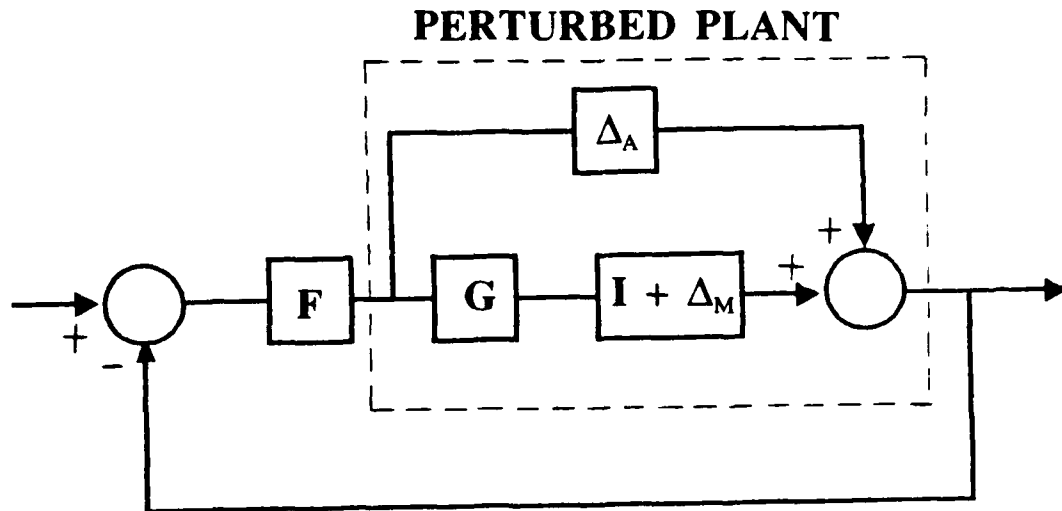


Figure 3.3 Additive / Multiplicative uncertainty

**Robustness Theorem 1:**

*If the system in Fig. 3.3 is stable as both  $\Delta_A$  and  $\Delta_M$  are zero. Let  $\Delta_A = 0$ , the size of the smallest stable  $\Delta_M(s)$  for which the system become unstable is*

$$\bar{\sigma}(\Delta(j\omega)) = \frac{1}{\bar{\sigma}(T(j\omega))}$$

Where  $T(j\omega)$  is the complementary sensitivity function of the system. It is seen that decreasing the value of  $\bar{\sigma}(T(j\omega))$  will increase the size of  $\Delta(j\omega)$ , that is, increase the stability margin.

**Robustness Theorem 2 :**

Suppose the system in Fig. 3.3 is stable when  $\Delta_A$  and  $\Delta_M$  are both zero. Let  $\Delta_M = 0$ . Then the size of the smallest stable  $\Delta_A(s)$  which destabilizes the system is

$$\bar{\sigma}(\Delta_A(j\omega)) = \frac{1}{\bar{\sigma}(\mathbf{R}(j\omega))} \quad [\text{Ref. 5}]$$

We can see that the smaller  $\bar{\sigma}(\mathbf{R}(j\omega))$  is, the greater will be the stability margin.

With properly selected weighting function matrices  $\mathbf{W}_2(j\omega)$  and  $\mathbf{W}_3(j\omega)$ , the stability margins of the control system can be specified by the following singular value inequalities,

$$\bar{\sigma}(\mathbf{R}(j\omega)) \leq | \mathbf{W}_2^{-1}(j\omega) |$$

$$\bar{\sigma}(\mathbf{T}(j\omega)) \leq | \mathbf{W}_3^{-1}(j\omega) |$$

Together with the performance specification  $\mathbf{W}_1(j\omega)$ , the design specifications of the robust control system may be written as

$$\bar{\sigma}(\mathbf{S}(j\omega)) \leq | \mathbf{W}_1^{-1}(j\omega) | \quad (3.3)$$

$$\bar{\sigma}(\mathbf{R}(j\omega)) \leq | \mathbf{W}_2^{-1}(j\omega) | \quad (3.4)$$

$$\bar{\sigma}(\mathbf{T}(j\omega)) \leq | \mathbf{W}_3^{-1}(j\omega) |. \quad (3.5)$$

Thus, for a robust control system synthesis, the requirements may be presented as reducing the plant disturbance effect as much as possible while meeting the control inputs and the robustness constraints. This goal can be achieved by the singular value loop shaping iterative procedure that will be introduced in the following sections.

As a consequence of singular value properties and the definition of  $H_\infty$  norm, these singular value inequalities can be combined into the single infinity norm specification in terms of the close loop transfer function  $\mathbf{T}_{y1u1}$  of the form

$$\| \mathbf{T}_{y|u} \|_{\infty} \leq 1$$

where

$$\mathbf{T}_{y|u} = \begin{bmatrix} \mathbf{W}_1 \mathbf{S} \\ \mathbf{W}_2 \mathbf{R} \\ \mathbf{W}_3 \mathbf{T} \end{bmatrix}$$

Note, the matrix  $\mathbf{T}_{y|u}$  is partitioned into submatrices representing performance requirements and stability constraints.

### C. WEIGHTING MATRIX SELECTION

Since the plant disturbance can be attenuated by reducing the value of  $\bar{\sigma}(s(j\omega))$  continuously, a constant scalar weighting gain  $\gamma$  is added to  $\mathbf{W}_1$  to facilitate the singular value loop shaping process. That is

$$\bar{\sigma}(S(j\omega)) \leq | \gamma^{-1} * \mathbf{W}_1^{-1}(j\omega) |$$

So, as we increase the value of  $\gamma$ , the sensitivity function is suppressed down continuously. On the other hand, from Eq. (2.9) ( $\mathbf{T}(s) + \mathbf{S}(s) = \mathbf{I}$ ), we know that  $\mathbf{T}(s)$  goes to  $\mathbf{I}$  as  $\gamma$  increases (since  $\mathbf{S}(s)$  goes to zero). This means the complementary sensitivity is forced against its upper constraint  $\mathbf{W}_3^{-1}(s)$  as the value of  $\gamma$  increases. The closed loop bandwidth, therefore, is widened. This improves the system performance, i.e., make system response faster. At the same time, the singular values of closed loop transfer function  $\mathbf{T}_{y|u}$  is pushed up to upper limit. The singular value loop shaping process stops as the condition in eq. (3.9) is reached.

It is interesting to note that,

$$\mathbf{S}(s) = (\mathbf{I} + \mathbf{L}(s))^{-1} \approx \mathbf{L}(s)^{-1}$$

as  $\underline{\sigma}(\mathbf{L}(j\omega)) \gg 1$ , ( i.e., the system has large loop gains)

i.e.,

$$1 / \bar{\sigma}(S(j\omega)) \approx \underline{\sigma}(L(j\omega))$$

Similarly, as  $\bar{\sigma}(L(j\omega)) \ll 1$ ,

$$T(s) = L(I + L(s))^{-1} \approx L(s)$$

that is,

$$\bar{\sigma}(T(j\omega)) \approx \bar{\sigma}(L(j\omega))$$

These can be seen in Fig. 3.4, i.e., above the zero dB line,  $\underline{\sigma}(L(j\omega)) \gg 1$ ,  $1 / \bar{\sigma}(S(j\omega)) \approx \underline{\sigma}(L(j\omega))$ , while below the zero dB line,  $\bar{\sigma}(L(j\omega)) \ll 1$ ,  $\bar{\sigma}(T(j\omega)) \approx \bar{\sigma}(L(j\omega))$ . Thus the robust system design consists of the use of high loop gains at low frequencies where the performance specifications are defined and the use of low loop gains at high frequencies where the robustness constraints lie [Refs. 5, 13]. The system performance will be limited within the range between  $\bar{\sigma}(G(s)F(s))$  curve and  $\underline{\sigma}(G(s)F(s))$  curve.

The weightings  $W_1$  and  $W_2$  are selected as transfer function matrices of which diagonal elements are frequency-dependent constants. And the size of these weighting matrices is the same as the number of plant output states. This small gain problem is solved by using a software program, i.e., "hinf.m" provided by MATLAB ROBUST-CONTROL TOOLBOX package. The number of states of the stabilizing controller  $F(s)$  produced by "hinf.m" is the same as that of  $P(s)$ . In addition it is required by "hinf" that the  $D_{12}$  submatrix of  $P(s)$  (see Eq. (3.1)) is full column rank. An easy way to ensure that this is the case is to choose the weighting matrix  $W_2$  with an invertible "D-matrix", e.g.,  $W_2(s) = \epsilon I$ , where  $\epsilon$  is any non-zero number [Ref. 5]. The parameters considered in selecting these weightings are gain, order, attenuation and corner frequency, which are used to achieve small  $\bar{\sigma}(S(s))$ , i.e., large loop gains,

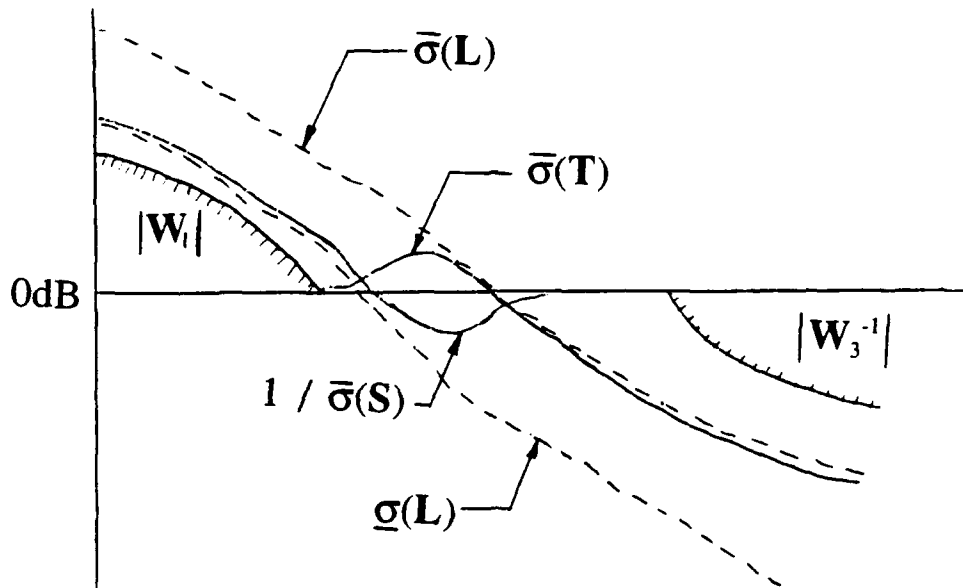


Figure 3.4 Singular Value Spec's on  $S(s)$  and  $T(s)$

over the broadest possible bandwidth subject to the robustness constraints. And it should be noted that the controller  $F(s)$  depends on the weighting matrices selected. Once the weightings are selected, the control system design is in a computer-aided design environment and requires only "one parameter"  $\gamma$ -iteration. The flow chart of the  $H_\infty$  iterative procedure is shown in Fig. 3.5.

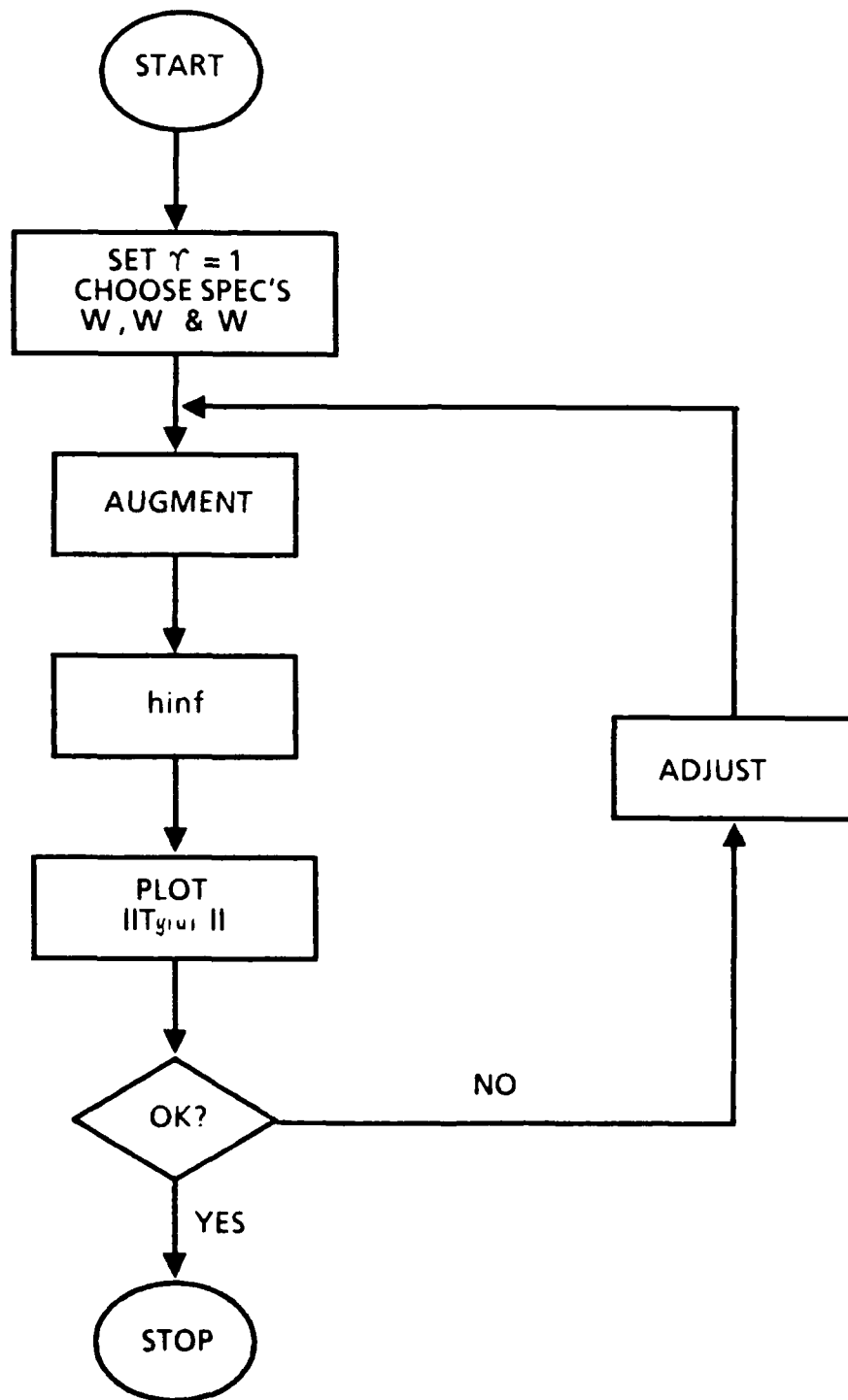


Figure 3.5  $H_\infty$  Singular Value Loop Shaping Iterative Process

#### IV. $H_2$ CONTROLLER SYNTHESIS FOR X-29 FIGHTER

The purpose of this Chapter is to present a modern aircraft controller design procedure based on the  $H_2$  optimal control theory. The model used is the longitudinal dynamic model of X-29 fighter. The X-29 is a single seat forward swept wing (FSW) demonstrator aircraft build by Grumman Co., which is designed to be a new generation of tactical fighter with the advantages of light weight, low cost and high efficiency. The computer-aided design program, MATLAB-ROBUST CONTROL TOOL BOX, is used in controller synthesis. The brief plant description and design objective are given in the following sections. The design procedure and results are also presented. The script files specifically written or modified for this problem are listed in appendix A.

##### A. PLANT DESCRIPTION

The aerodynamic advantages of forward swept wing design include improved maneuverability, with virtually spin-proof characteristics, better low-speed handling and reduced stalling speed. The FSW X-29 (see Fig. 4.1) was selected primarily because its multiple, independently controlled surface make it an ideal candidate for multiloop synthesis of advanced control mode.

The aircraft is designed to have a -35% stability margin at subsonic speed. A wing strake extends aft from the trailing-edge at each wing root, each strake with a trailing-edge flap which has its own integrated servo actuator to augment foreplanes for pitch control. All-moving canard surfaces, one on each side of the center fuselage, outboard of engine inlet ducts and operated by servo actuators for primary pitch

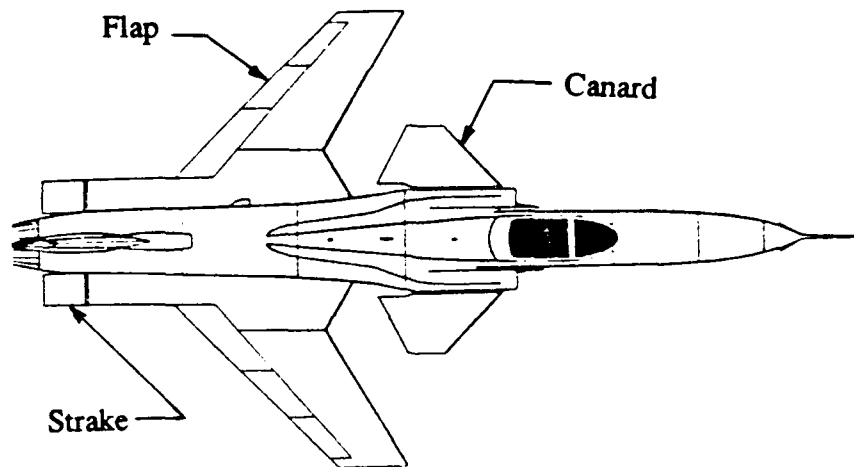


Figure 4.1 FSW X-29 Fighter

control. In addition the aircraft is equipped with flaperons [Ref. 10].

The X-29 longitudinal dynamic model considered in this study is an analog reversion mode with the aircraft trimmed at 0.5 mark, 30,000 feet. The design point was one of the critical nodes in the analysis of the aircraft. The 14-state reduced-order model includes a short period approximation of the aircraft longitudinal dynamics, vertical velocity  $w$  and pitch rate  $q$ , and 3 fourth order actuator dynamics for the longitudinal control surfaces respectively, i.e., the canards, flaperons and strakes.

For the first design, a 2-input, 2-output configuration is used. Two separated commands  $r_1$  and  $r_2$  are input to the three control surface actuators with  $r_1$  controlling the canards and strakes and  $r_2$  controlling the flaps. The outputs of the system are two

aircraft states,  $w$  and  $q$ . The physical configuration of this 2-input, 2-output open loop actuator/aircraft dynamics model is shown in Fig. 4.2.

The second design example considered is a 3-input, 3-output controller synthesis. Three separated commands  $r_1$ ,  $r_2$  and  $r_3$ , are input to the three control surfaces canards, flaps and strakes respectively. The output to be controlled are  $w$ ,  $q$  and the canard control input  $\delta_c$ . The physical configuration for this model is shown in Fig. 4.3. Comparison is made between this two proceeding designs.

The state variables are listed in Table 4.1. The state space realization of the open loop plant model  $G$  is listed in Appendix B. The poles of this system are listed in Table 4.2. It is seen that there is a positive pole, i.e., 1.9550, on the real axis. That means the X-29 has an unstable short period mode.

The 14-state model was scaled to improve the numerical conditioning of its state space representation. The  $w$  state was transformed to angle of attack  $\alpha$  using the initial forward velocity  $u_0$ , i.e.,  $\alpha = w / u_0$ . The units of the actuator third derivative states were transformed from  $\text{rad}/\text{sec}^3$  to  $1\text{e}+04 \text{ rad}/\text{sec}^3$ . This scaling was effective in reducing the condition number of the system state matrix  $A_g$  from an order of magnitude of  $10^{10}$  to  $10^4$  [Ref. 13].

The singular value plot of the uncompensated plant  $G(s)$  is presented in Fig. 4.4. The solid curve and dashed curve represent the maximum and minimum singular values of  $G(s)$  respectively. As can be seen, at low frequency, the open loop plant has poor disturbance attenuation, high sensitivity to plant variations and modeling errors, and a small control bandwidth. These properties will be improved by singular value loop shaping procedure presented in the following sections.

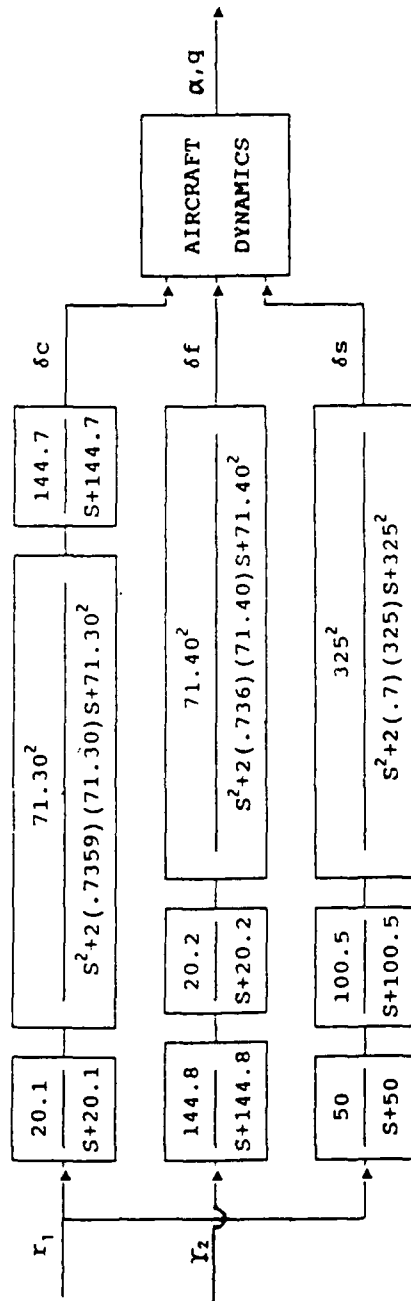


**Figure 4.2** X-29 2-Input, 2-Output Open Loop Configuration  
 Source : W. L. Rogers [Ref. 13]

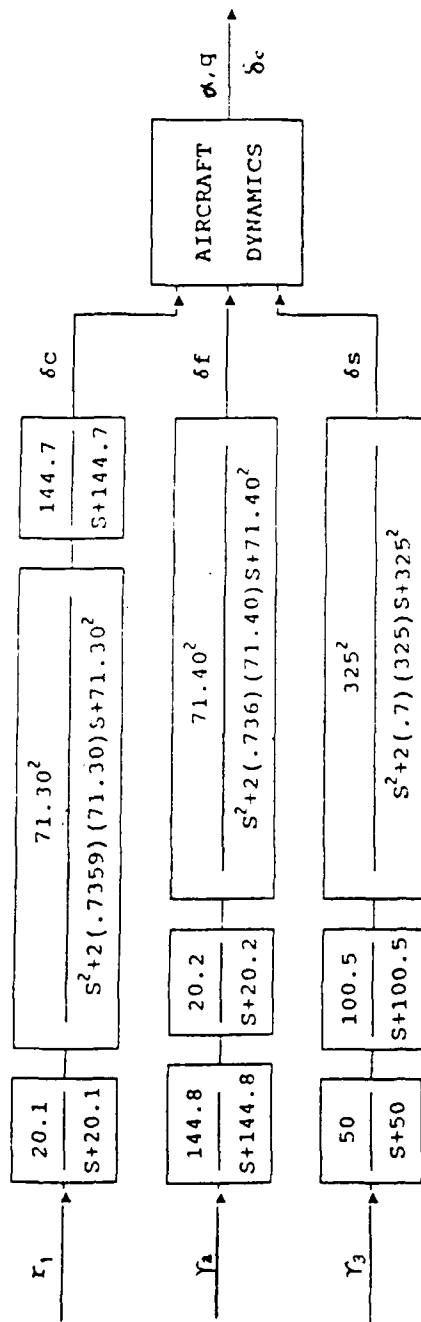


Figure 4.3 X-29 3 I/O Open Loop Configuration  
 Source : W. L. Rogers [Ref. 13]

**Table 4.1** Discription of The Uncompensated X-29 state variables

<u>State</u>	<u>Description</u>	<u>Units</u>
$\alpha$	angle-of-attack	rad
$q$	pitch rate	rad/sec
$\delta_c$	canard control input	rad
$\delta_f$	flap control input	rad
$\delta_s$	strake control input	rad
$\dot{\delta}_c$	canard control rate	rad/sec
$\dot{\delta}_f$	flap control rate	rad/sec
$\dot{\delta}_s$	strake control rate	rad/sec
$\ddot{\delta}_c$	canard control accel.	rad/sec <sup>2</sup>
$\ddot{\delta}_f$	flap control accel.	rad/sec <sup>2</sup>
$\ddot{\delta}_s$	strake control accel.	rad/sec <sup>2</sup>
$\delta_c^{\prime\prime\prime}$	canard control jerk	1e+04 rad/sec <sup>3</sup>
$\delta_f^{\prime\prime\prime}$	flap control jerk	1e+04 rad/sec <sup>3</sup>
$\delta_s^{\prime\prime\prime}$	strake control jerk	1e+04 rad/sec <sup>3</sup>

Source : W. L. Rogers [Ref. 13]

**Table 4.2** Uncompensated X-29 open loop poles

```

poleg =
      -2.2746e+02 + 2.3201e+02i
      -2.2746e+02 - 2.3201e+02i
      -1.4455e+02
      -1.4491e+02
      1.9550e+00
      -1.0031e+02
      -2.7155e+00
      -5.2518e+01 + 4.8255e+01i
      -5.2518e+01 - 4.8255e+01i
      -5.2506e+01 + 4.8410e+01i
      -5.2506e+01 - 4.8410e+01i
      -5.0067e+01
      -2.0172e+01
      -2.0115e+01
  
```

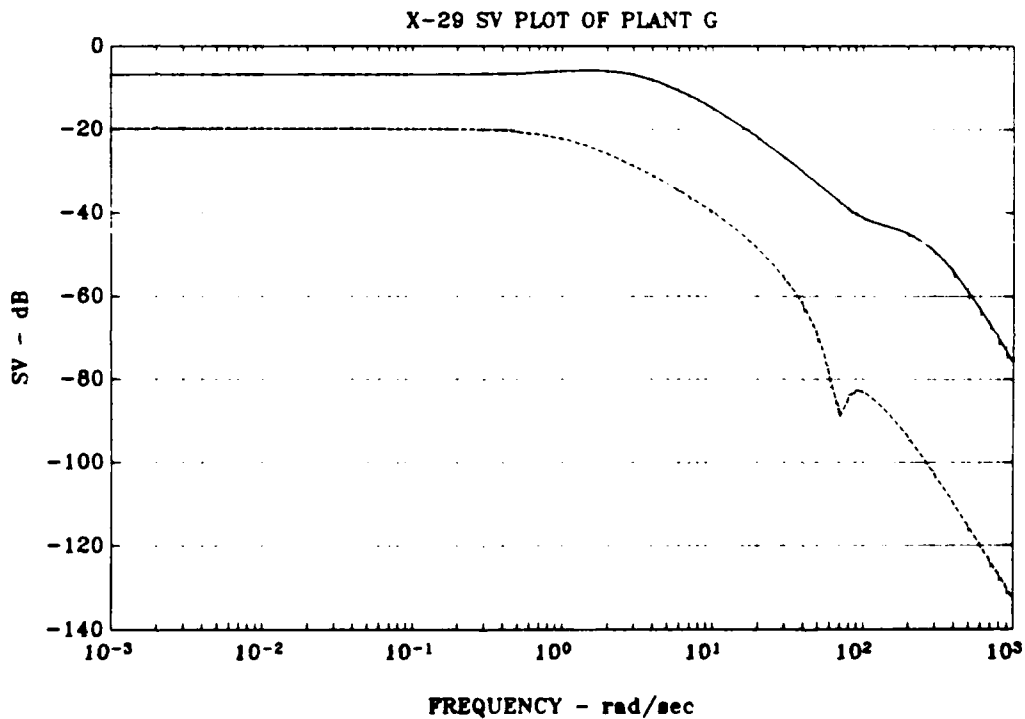


**Figure 4.4** Singular Value Plot of The Uncompensated Plant G(s)

## B. DESIGN SPECIFICATIONS AND WEIGHTING FUNCTIONS

Since the design objective is to attenuate the disturbance effect as much as possible within loop gain constraint and robustness specifications. The design specifications, in this case, are :

Performance Spec.:

Minimize the sensitivity function as much as possible.

Robustness Spec.:

- 1). Attenuate the close-loop singular values of the complementary sensitivity matrix by 20 db at frequencies beyond  $\omega = 100$  rad/sec (15.9 Hz) (This will ensure that the system will have sufficient stability margin to tolerate variations the loop transfer function of magnitude as large as a factor of ten at frequency  $\omega = 100$  rad/sec).
- 2). a second-order roll-off beyond  $\omega = 100$  rad/sec (This ensures the controller is proper and matches the uncontrolled drop-off).

With these considerations, we have covered the most important issue in feedback control system design. Once the design specifications are decided, the selection of weighting matrices is the next step. For the 2-input 2-output system, the weighting matrices are chose as follows :

$$(\gamma W_1(s))^{-1} = \gamma^{-1} * \frac{.01 ( 1 + s / .01 )}{( 1 + s / 100 )} * I \quad (2 \times 2) \quad (4.1)$$

$$W_2(s) = - 0.025 * I. \quad (4 \times 4) \quad (4.2)$$

$$W_3^{-1}(s) = \frac{1000}{s^2} * I \quad (4.3)$$

(2 x 2)

to penalize the error " e ", control input " u " and output " y " respectively.

The singular value plot of  $W_1^{-1}(s)$ ,  $W_3^{-1}(s)$  weighting functions is given in Fig. 4.5. The robustness specification  $W_3^{-1}(s)$  has 20 dB drop-off and 40 dB roll-off at  $\omega = 100$  rad/sec which satisfied the design requirements. As mentioned,  $W_1^{-1}(s)$  and  $W_3^{-1}(s)$  should be so chose to ensure the 0 dB crossover frequency of  $W_1$  is sufficiently lower than the 0 dB crossover frequency of  $W_3^{-1}(s)$ .  $W_2(s)$  is selected to penalize the

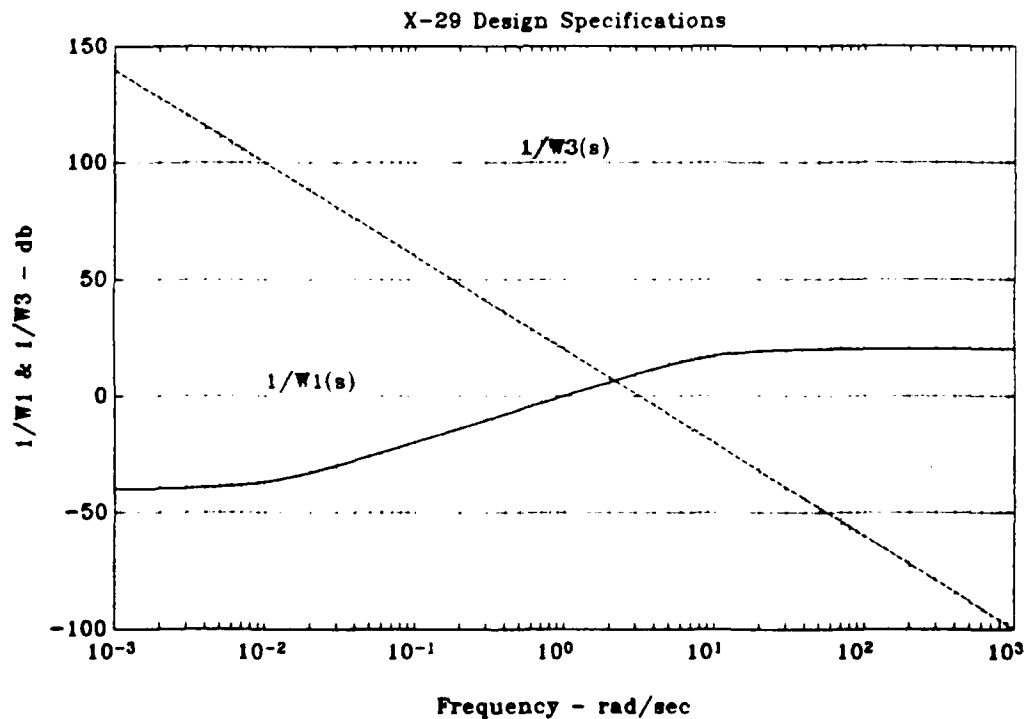


Figure 4.5 Singular Value Plot of Weighting Functions

control input  $u$ , and the weighting factor 0.025 is chosen to confine the actuators' response within their design limits. The selected  $W_2(s)$  also ensures that the submatrix  $D_{12}$  of  $P(s)$  has full column rank as required in the two Riccati equation solution to the  $H_\infty$  problem. The  $H_\infty$  theory requires that  $D_{12}(s)$  matrix is full column rank in order for an optimal  $H_\infty$  controller to eliminate infinite energy inputs. If we decrease the weighting factor, more energy will input to the system, in this case, the actuators' response may exceed the limits [Ref. 13].

### C. DESIGN PROCEDURE

Before starting the singular value loop shaping procedure, it is necessary to find the balanced state space realization for the unaugmented plant for a better numerical condition. This can be seen from the different condition numbers of state matrix  $A_g$  before and after balanced realization, which are  $5.526e+04$  and  $2.5567e+02$  respectively.

#### 1. 2-INPUT, 2-OUTPUT DESIGN CASE

With the selected weighting matrices, the augmented plant  $P(s)$  of the balanced plant is of order eighteenth,  $W_1(s)$  and  $W_2$  each adding two states to the system  $G(s)$ . Since  $W_3(s)$  is not a proper transfer function Eq. (4.3) (i.e., it has more zeros than poles), so it has no state space realization. But  $W_3(s)G(s)$  is proper and can be realized in state space form.

With the computer-aided design program,  $\gamma$  is chosen as 1 for the first try of the iteration process. As continuously increasing the value of  $\gamma$ , the singular value of cost function  $T_{y|u}$  is pushed up to its upper limit gradually until no solution exists for any larger  $\gamma$ . After several iterations,  $\gamma$  equals to 2.6, and the maximum singular values of  $T_{y|u}$  reached the all pass limit (i.e., 0 dB line). Fig. 4.6 is the singular value

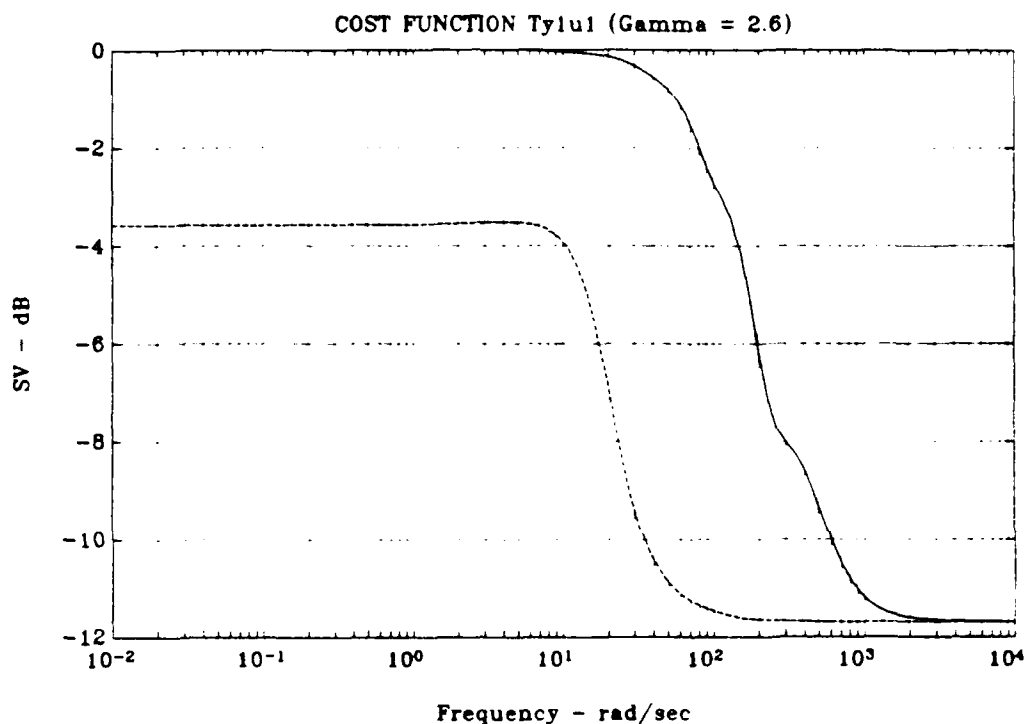


Figure 4.6 Cost Function  $T_{y|u}$  for  $\gamma = 2.6$

plot of cost function  $T_{y|u}$ , the solid line represents the maximum singular values and dashed line represents the minimum singular values. Fig. 4.7 and 4.8 are the singular value plots of complementary sensitivity and sensitivity, the dashed line and dotted line again represent the maximum and minimum singular values respectively. The complementary function is pushed flat against the specified limit  $W_s^{-1}$ , as the value of gamma is increased, the closed loop bandwidth is widened (to 30 rad/sec) and the response speed is increased. Similarly, the sensitivity function is pushed down against its limit  $\gamma^{-1}W_1^{-1}$  as  $\gamma$  value increased. The singular value of  $I + G(s)F(s)$  loop gains are increased to about 50 dB at low frequency for this design, which markedly improves the X-29 performance properties. This large loop gains indicate good disturbance attenuation and low sensitivity to plant variations over a control bandwidth

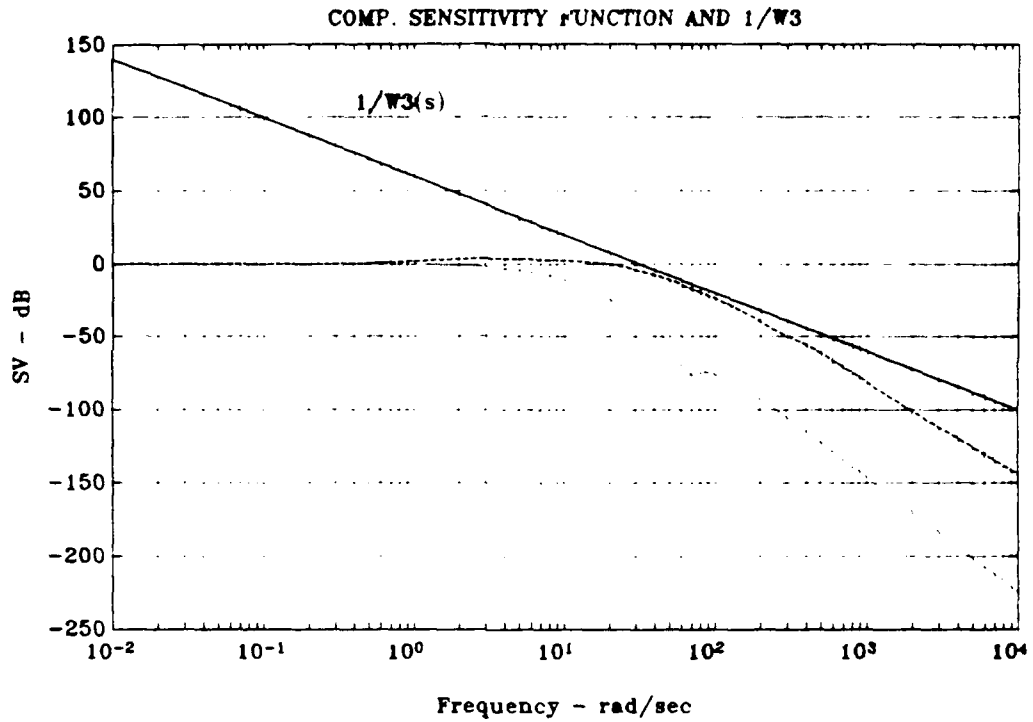


Figure 4.7 Complementary Sensitivity Function  $T(s)$  and  $W_3^{-1}$  for  $\gamma = 2.6$

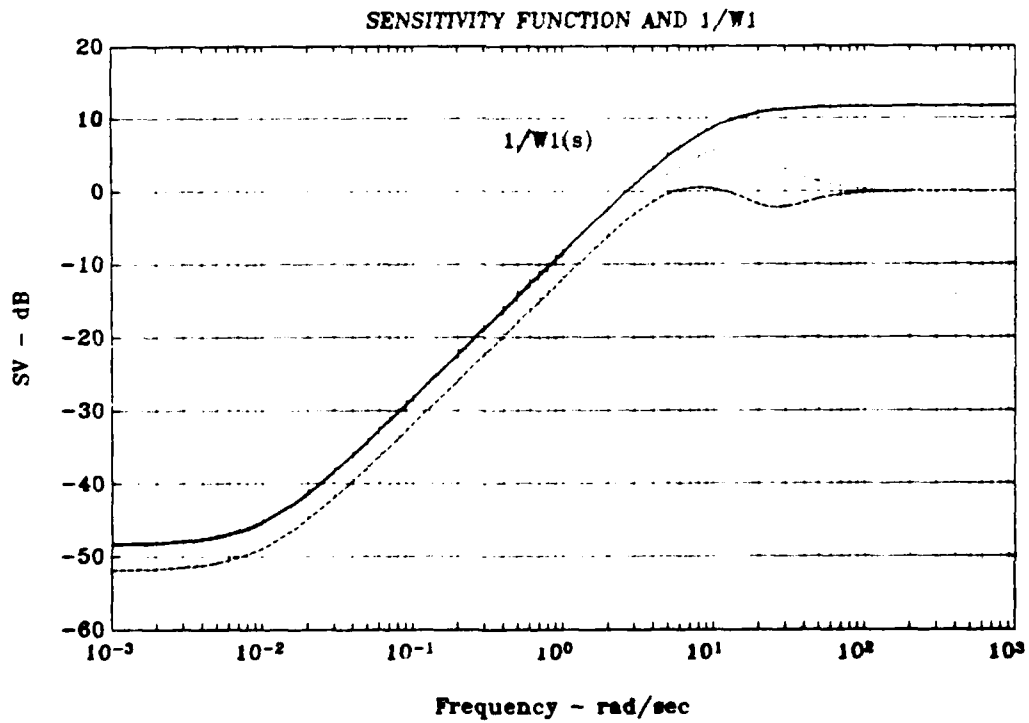


Figure 4.8 Sensitivity Function  $S(s)$  and  $W_1^{-1}$  for  $\gamma = 2.6$

of about 3 rad/sec and satisfy the stability requirements. Note, in Fig. 4.8,  $W_1^{-1}(s) = \bar{\sigma}(S(j\omega))$  at low frequency. And there is about 40 dB drop-off from  $\omega = 10$  rad/sec to  $\omega = 0.1$  rad/sec which is the range of interesting. The state space realization of the 18-state stabilizing controller  $F(s)$  is listed in Appendix C. Two uncontrollable states are removed using PRO-MATLAB function "minreal.m". A fast transient poles is eliminated while retaining the most important characteristics of the closed loop system. Thus, the final controller has 15 states. The poles of this reduced-order controller are listed in Table 4.3.

**Table 4.3** Poles of The Reduced-Order Controller

```
poleacpr =
-2.1954e+02
-6.5170e+01 + 9.5444e+01i
-6.5170e+01 - 9.5444e+01i
-1.4487e+02
-1.3577e+02
-5.3024e+01 + 4.9271e+01i
-5.3024e+01 - 4.9271e+01i
-4.1572e+01 + 3.1587e+01i
-4.1572e+01 - 3.1587e+01i
-1.3180e+01 + 1.9602e+01i
-1.3180e+01 - 1.9602e+01i
-3.0118e+01 + 1.8361e+01i
-3.0118e+01 - 1.8361e+01i
-1.0000e-02
-1.0000e-02
```

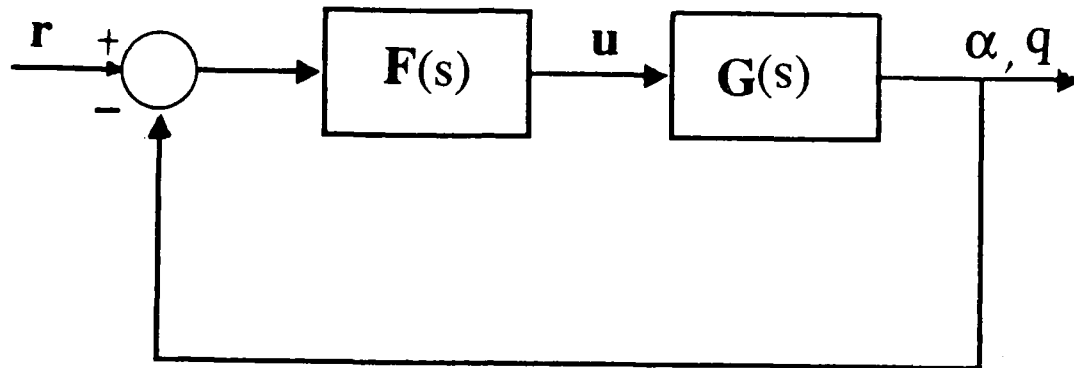


Figure 4.9 X-29 Feedback Configuration

Fig. 4.9 shows the closed loop system of compensated X-29, where  $F(s)$  is the 15th order controller and  $G(s)$  is the 14th order X-29 plant. Since  $F(s)$  is placed in series with plant  $G(s)$ , the command vector  $r$  is composed of the reference commands  $r_1$  and  $r_2$  to controlled outputs  $\alpha$  and  $q$ . So, the closed loop compensated system has 2 inputs, 2 outputs and 29 states. The poles of this reduced-order closed loop system are listed in Table 4.4. The singular value plot of output, inverse-return difference matrix  $I + (G(s)F(s))^{-1}$  (also called the output, multiplicative return difference matrix) for the compensated system is shown in Fig. 4.10. The minimum singular value of this matrix, i.e.,  $\sigma_{\min}[I + (G(j\omega)F(j\omega))^{-1}]$ , provides a measure of the aircraft's gain and phase margins with respect to multiplicative modeling errors using the universal gain and phase margin curve (Fig.4.11) [Ref. 4].

**Table 4.4 Poles of The 2 I/O Closed Loop System**

```

-2.2739e+02 + 2.3194e+02i
-2.2739e+02 - 2.3194e+02i
-2.1723e+02
-6.4876e+01 + 9.6310e+01i
-6.4876e+01 - 9.6310e+01i
-1.3558e+02
-1.4595e+02
-1.4469e+02 + 9.2844e-02i
-1.4469e+02 - 9.2844e-02i
-1.1118e+02
-4.9782e+01 + 4.9587e+01i
-4.9782e+01 - 4.9587e+01i
-5.2188e+01 + 4.8038e+01i
-5.2188e+01 - 4.8038e+01i
-5.2464e+01 + 4.8363e+01i
-5.2464e+01 - 4.8363e+01i
-4.1968e+01 + 3.2086e+01i
-4.1968e+01 - 3.2086e+01i
-4.1045e+01
-2.7932e+01 + 1.3447e+01i
-2.7932e+01 - 1.3447e+01i
-1.1994e+01 + 1.1959e+01i
-1.1994e+01 - 1.1959e+01i
-1.9603e+00
-2.6697e+00
-3.8935e+00
-1.0123e+01
-1.6232e+01
-1.9727e+01

```

It is seen in Fig. 4.10 that  $\sigma_{\min}[\mathbf{I} + (\mathbf{G}(s)\mathbf{F}(s))^{-1}]$  drops to about -3 dB at frequencies between 0.3 rad/sec and 20 rad/sec. Entering the vertical axis of the universal curve at singular value of 0.71 (i.e., -3 dB). The gain and phase margins of compensated X-29 near 0 dB crossover frequency are -11 dB to +5 dB and  $\pm 42$  deg respectively. This is more stable than the -8 dB to +4 dB and  $\pm 35$  deg gain and phase margins for the typical design of a fighter aircraft.

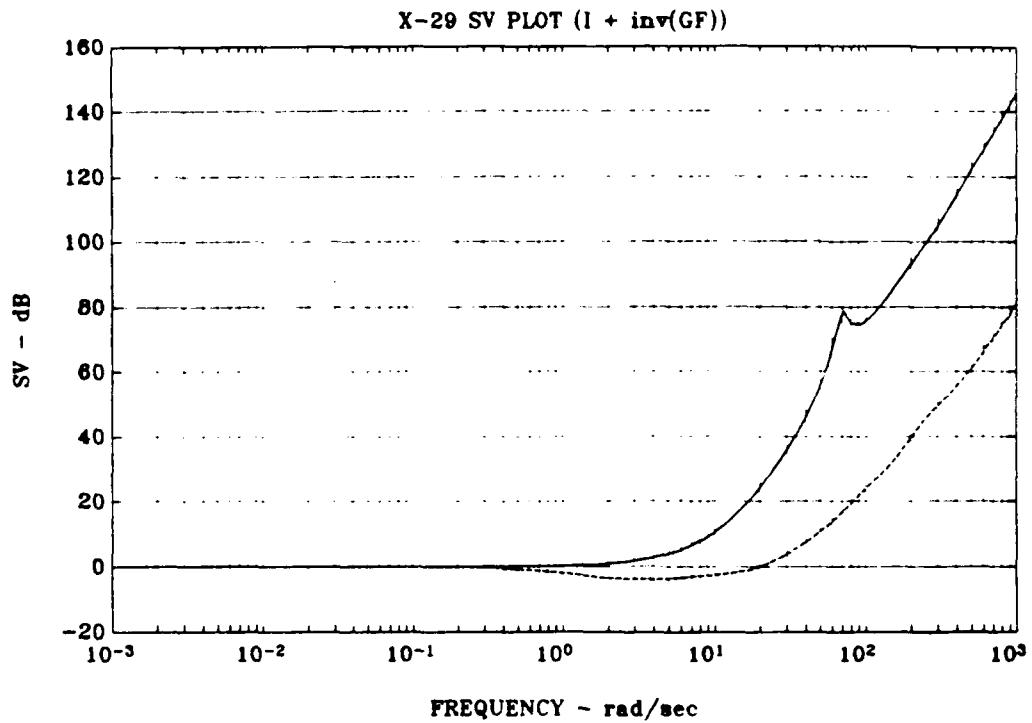


Figure 4.10 Singular Value Plot of The Output Inverse-Return Difference Matrix for 2 I/O System

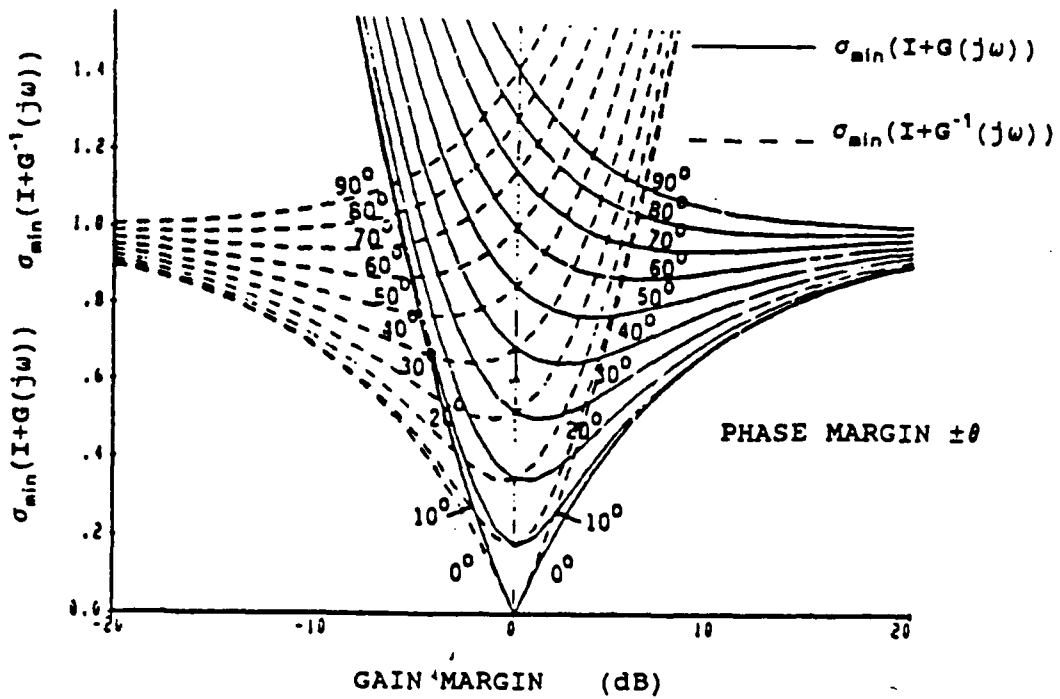


Figure 4.11 Universal Gain and Phase Margin Curve

Shown in Fig. 4.12 are the closed loop Bode plots of  $\alpha$  and  $q$  respectively. The solid curves are the response to  $r_1$ , and dashed curves are to  $r_2$ . It is seen that, at low frequency,  $\alpha$  is "all pass" (i.e., has 0 dB gain) to input 1 but has very small response (-50 dB) to input 2. Similarly, as seen that  $q$  is "all pass" to  $r_2$  but has small response to  $r_1$ . This indicates the decoupling of  $\alpha$  from  $q$  to  $r_1$  and  $r_2$ . Note, the system performance at high frequencies satisfy the robustness requirements for both cases.

The time response of  $\alpha$  and  $q$  to 1 deg/sec (0.01745 rad/sec) step input are presented in Fig. 4.13 and 4.14. It is seen from Fig. 4.13 that the response of  $\alpha$  is fast while with rise time of 0.3 seconds and 0.1 second to  $r_1$  and  $r_2$  respectively. We also can see that the decoupling of  $\alpha$  and  $q$  to the two commands from both plots. If we reduce the weighting function  $W_2(s)$ , more energy will be input to system, and that energy increases the response speed and the decoupling will be more pronounced.

Referring to Fig. 4.15 and 4.16, the time response of control deflections  $\delta_c$ ,  $\delta_f$ , and  $\delta_s$ . It is seen that the peak magnitudes are 0.013 rad, 0.006 rad, and 0.007 rad for  $\delta_c$ ,  $\delta_f$ , and  $\delta_s$  respectively, which are well within the X-29's control surface deflection limits listed below :

- (1). canards (leading edge) : 30 deg up / 60 deg down,
- (2). flaps (trailing edge) : 10 deg up / 25 deg down,
- (3). strakes (trailing edge) : 30 deg up and down.

The peak control rates (see Fig. 4.17 and 4.18) are 0.0013 rad/sec, 0.0004 rad/sec, and 0.0008 rad/sec respectively, which are much smaller than the X-29 actuator minimum design requirements of

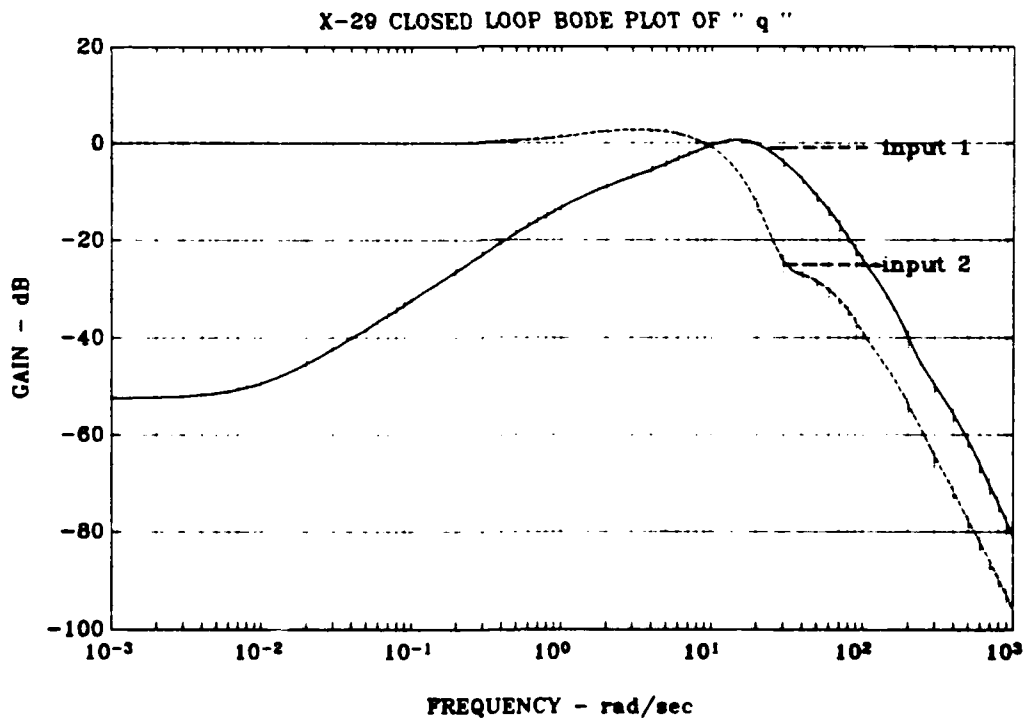
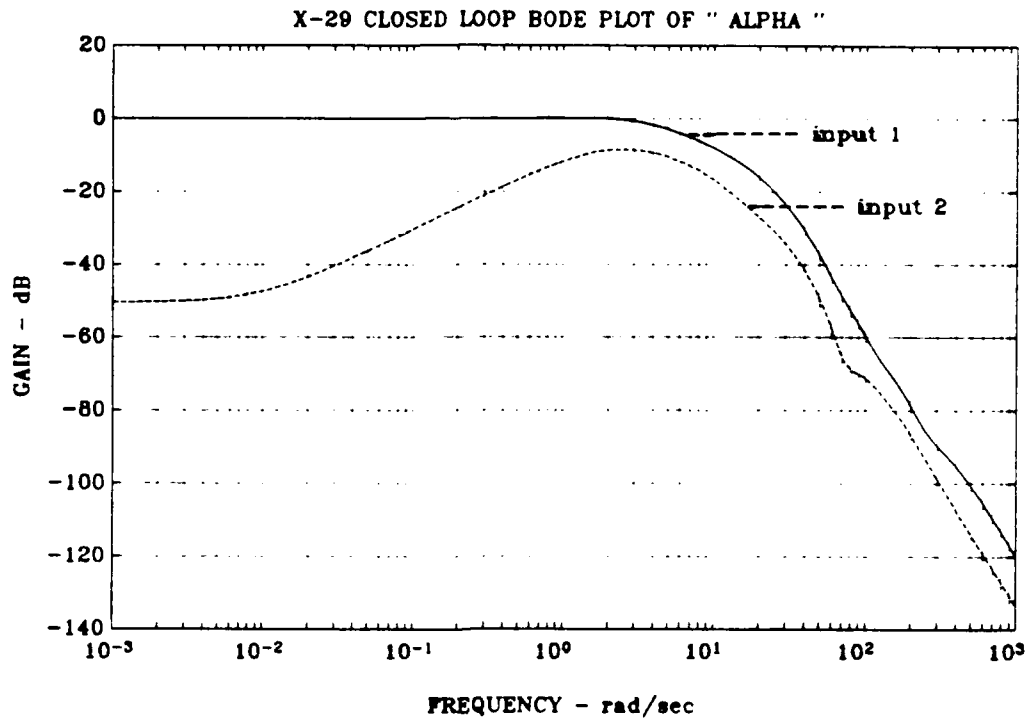


Figure 4.12 Closed Loop Bode Plot of  $\alpha$  and  $q$  for 2 I/O System

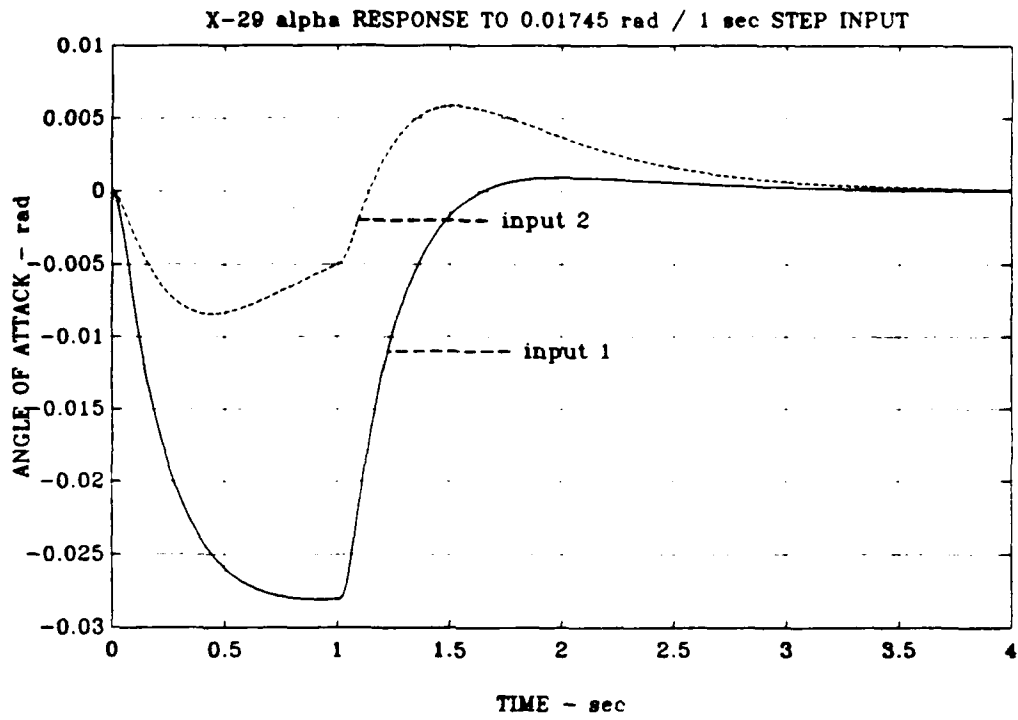


Figure 4.13 Step Response of  $\alpha$  for 2 I/O System

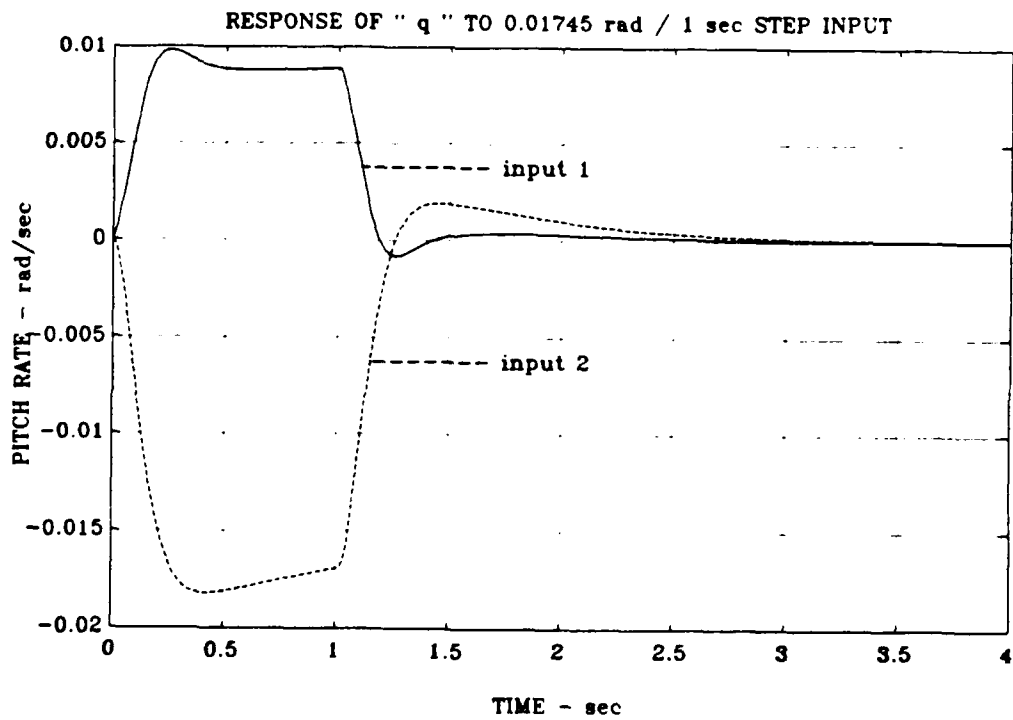


Figure 4.14 Step Response of  $q$  for 2 I/O System

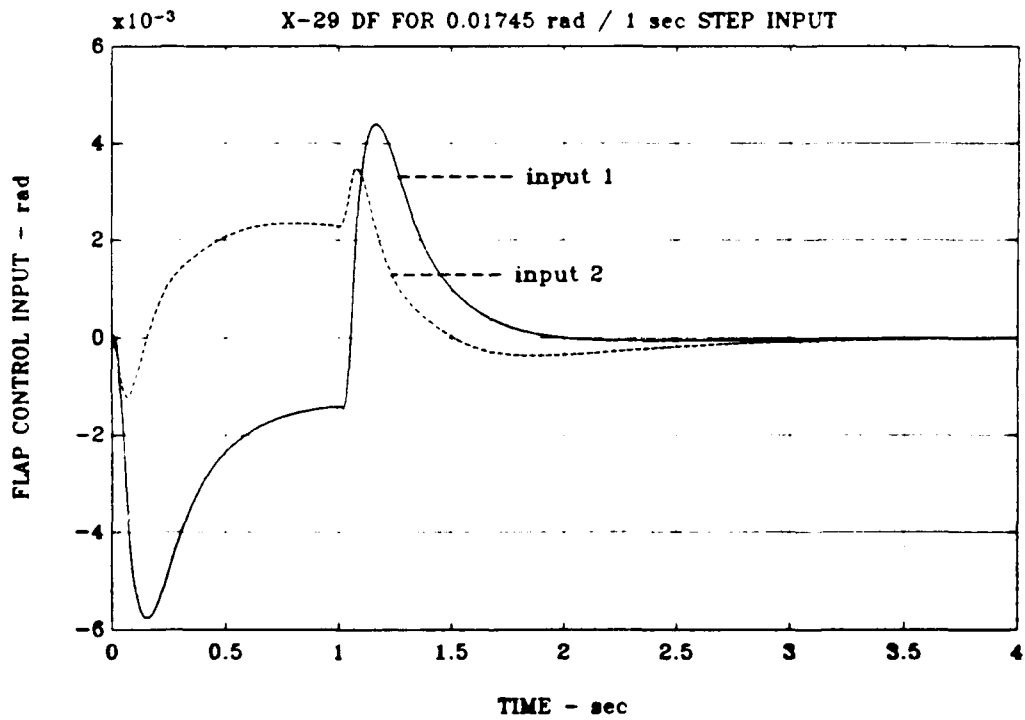
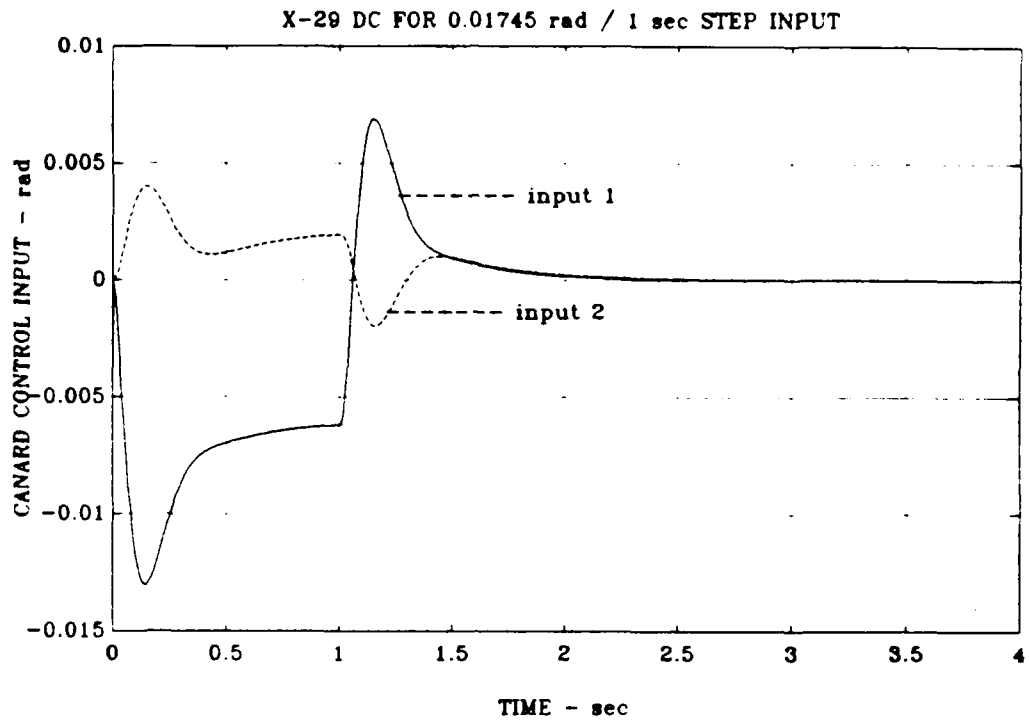


Figure 4.15 Step Response of Canard Control Input  $\delta_c$  and Flap Control Input  $\delta_f$

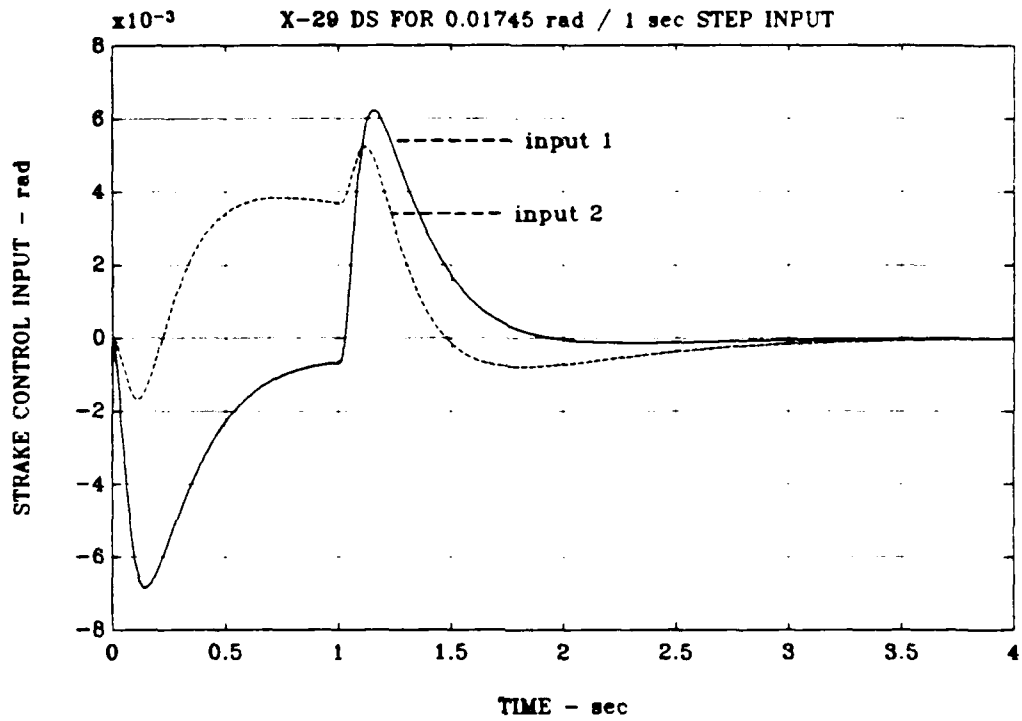


Figure 4.16 Step Response of Strake Control Input  $\delta_s$

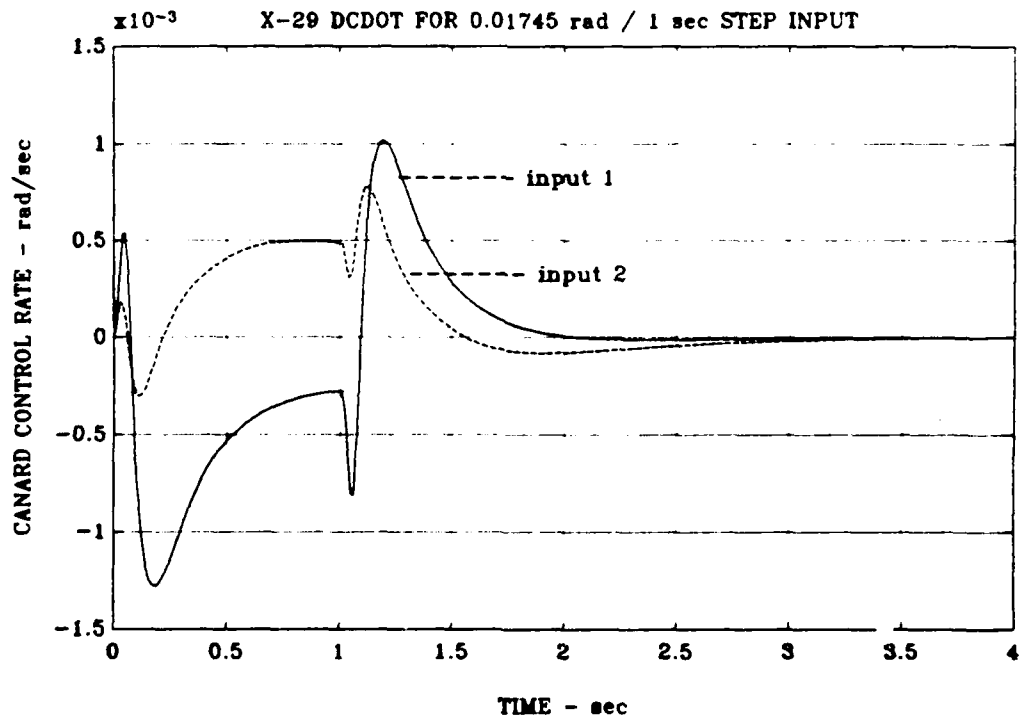


Figure 4.17 Step Response of Canard Control Rate  $\dot{\delta}_c$

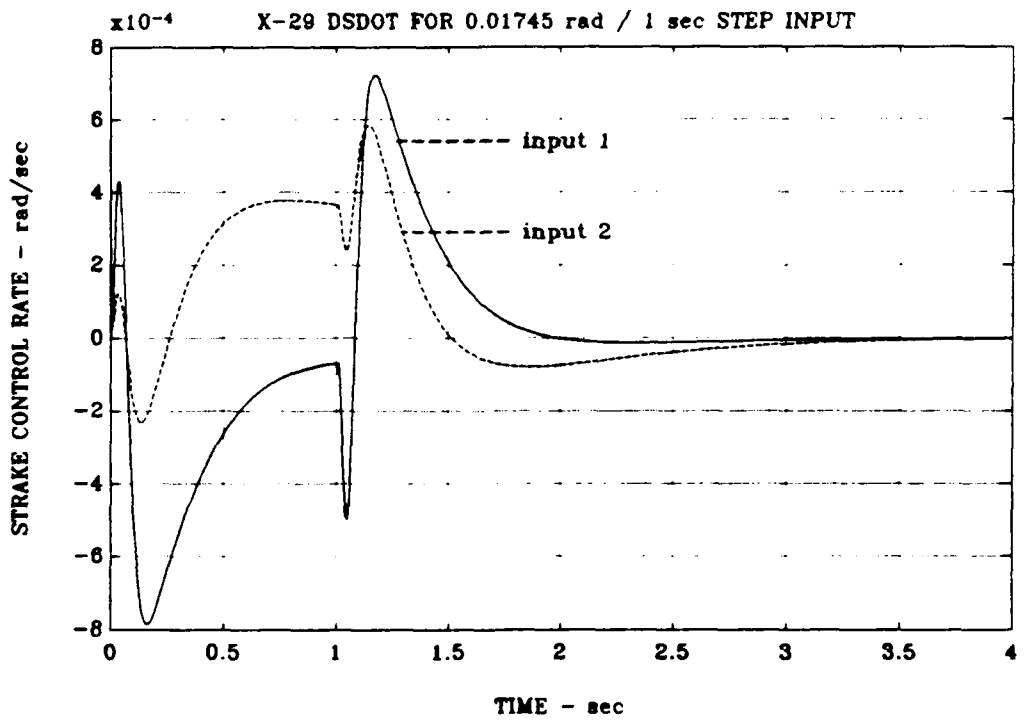
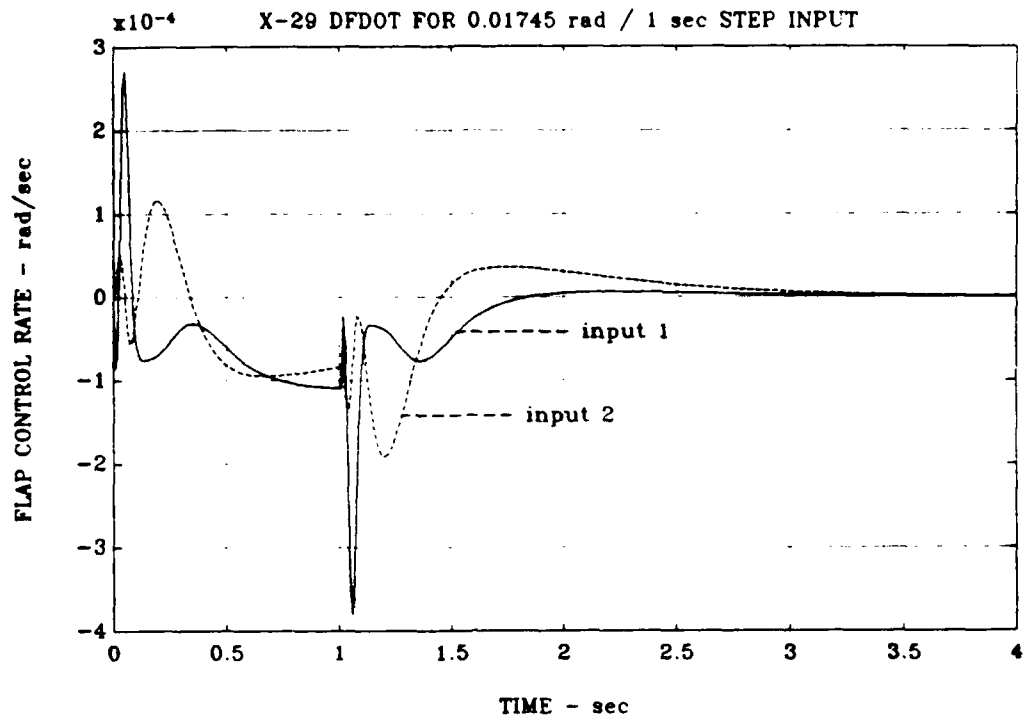


Figure 4.18 Step Response of  $\dot{\delta}_r$  and  $\dot{\delta}_s$

- (1). canards : 1.75 rad/sec
- (2). flaps : 0.87 rad/sec
- (3). strakes : 0.52 rad/sec.

The response is well within the actuator limits but one also has a very small step-input.

## 2. 3-INPUT, 3-OUTPUT DESIGN CASE

The second design example we use is the same X-29 dynamic model as in the previous example, but with different input and output vectors, i.e.,  $r_1$ ,  $r_2$ , and  $r_3$  to control canards, flaps and strakes separately and outputs are  $\alpha$ ,  $q$ , and  $\delta_c$  (see Fig. 4.3). Thus, it is a 3-input, 3-output system with 14 states.

The same design specifications are used for this case, and the weighting functions are chose as follows :

$$(\gamma W_1(s))^{-1} = \gamma^{-1} * \frac{.01 ( 1 + s / .01 )}{( 1 + s / 100 )} * \mathbf{I} \quad (3 \times 3) \quad (4.4)$$

$$W_2(s) = -0.025 * \mathbf{I} \quad (6 \times 6) \quad (4.5)$$

$$W_3^{-1}(s) = \frac{1000}{s^2} * \mathbf{I} \quad (3 \times 3) \quad (4.6)$$

The augmented plant  $P(s)$  is an 20th order system with  $W_1(s)$  and  $W_2(s)$  each adding three states to the plant  $G(s)$ . Following the same iterative procedure as of the previous example, the cost function reaches its all pass limit as  $\gamma = 1.3$  (see Fig. 4.19),

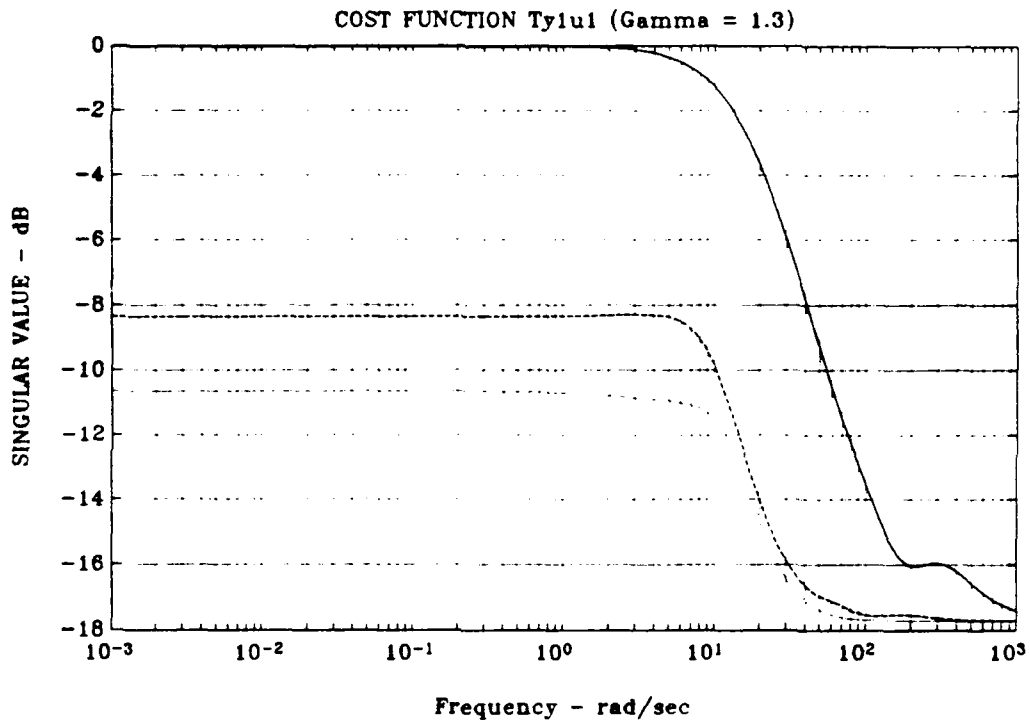


Figure 4.19 Cost Function  $T_{y|u}$  for  $\gamma = 1.3$

then the iterative process stops. The solid, dashed, and dotted curves in this plot represent the maximum, medium, and minimum singular values of  $T_{y|u}$  respectively. The controller  $F(s)$  produced has 20 states, that is the same as number of states of  $P(s)$ . Three states are removed using "minreal.m" function and one state is eliminated by "obalreal.m" program. So, the final controller has 16 states, the controller / plant series has 30 states in total (uncompensated plant  $G(s)$  has 14 states). The poles of this reduced-order closed loop system are listed in Appendix E. Comparing Fig. 4.20 with Fig. 4.7 and 4.8 shows that this 3 I/O system are not as robust as the 2 I/O model. The 3 I/O system has smaller disturbance attenuation, larger sensitivity to plant variations and modeling errors, smaller control bandwidth and closed loop bandwidth. Fig. 4.21 is the singular value plot of output, inverse-return

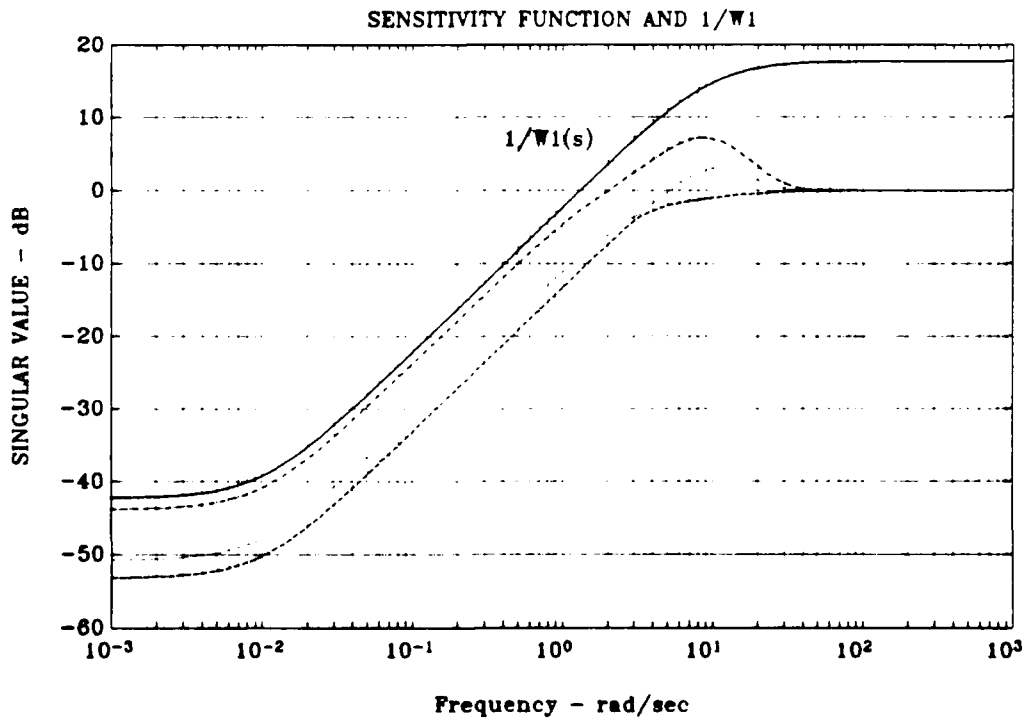
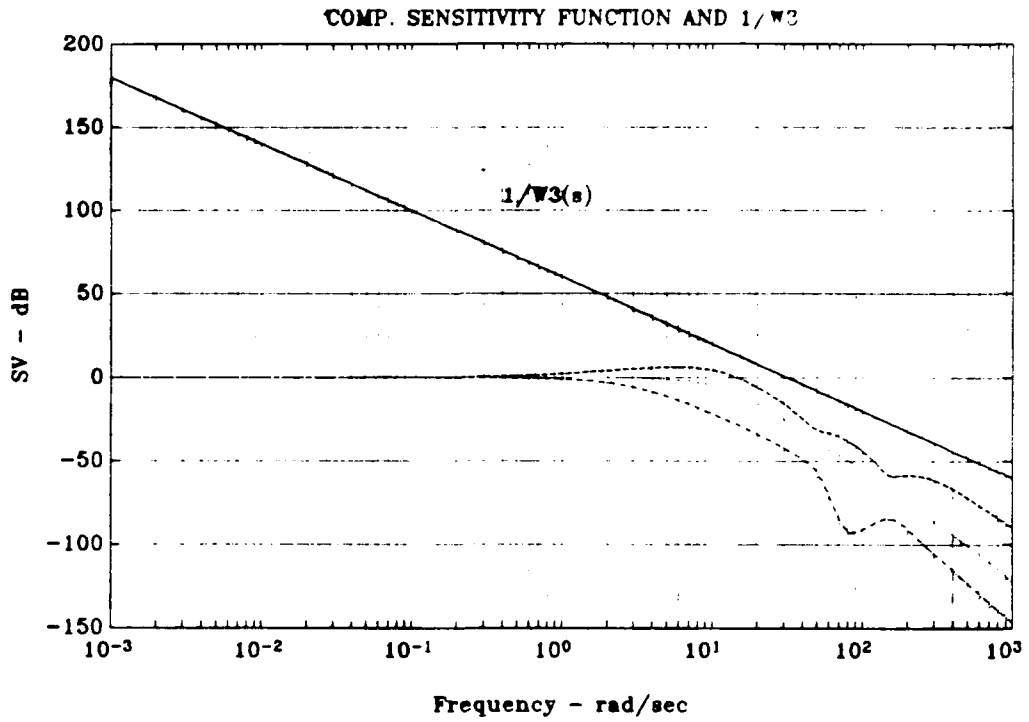


Figure 4.20 Complementary Sensitivity  $T(s)$  and Sensitivity  $S(s)$  for  $\gamma = 1.3$

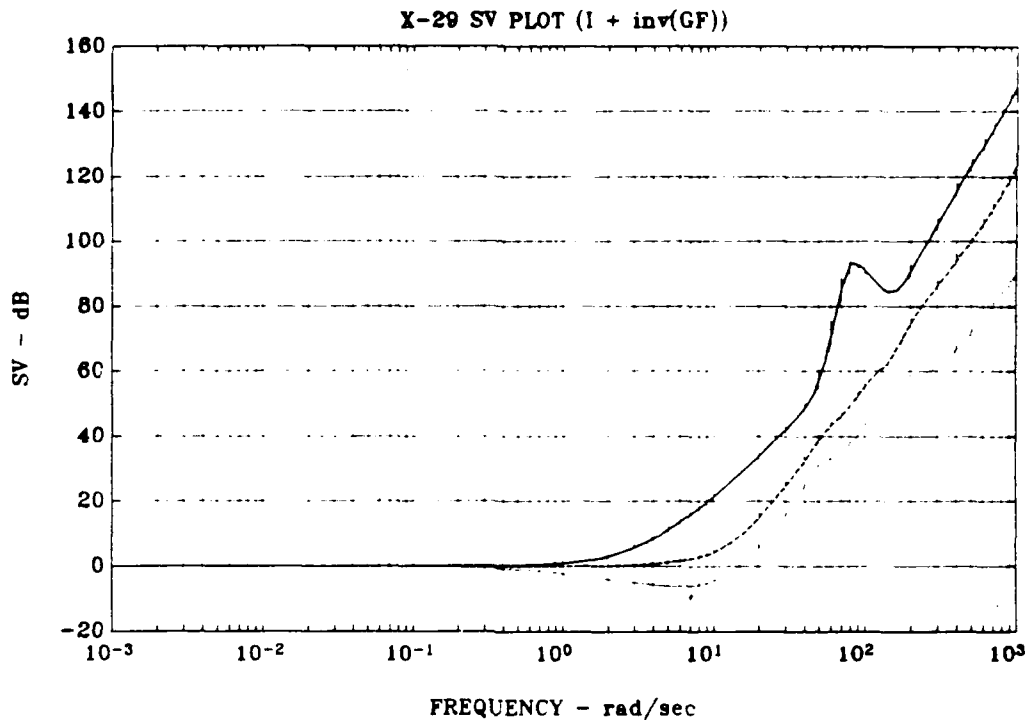


Figure 4.21 Output, Inverse Return Difference Matrix for 3 I/O System

difference matrix. It is seen that the  $\sigma_{\min}[ I + ((G(s)F(s))^{-1} ]$  (i.e., the dotted curve) drops to approximately -6 dB between 0.2 rad/sec and 13 rad/sec. Enter the vertical axis of the universal curve (Fig. 4.11) at singular value of 0.5 (i.e., -6 dB), the gain and phase margins near 0 dB crossover frequency are -6 dB to +3 dB and  $\pm 28$  deg respectively. It indicates that the stability margins of the 3 I/O system, with respect to multiplicative modeling errors, are less than the values desired of a fighter aircraft, i.e., -8 dB to +4 dB,  $\pm 35$  deg gain and phase margin respectively. Obviously, it is also not as stable as the 2 I/O system discussed before.

From Fig. 4.22, the Bode plots of  $\alpha$  and  $q$  to the 3 inputs, we also can see that  $\alpha$  is decoupled from  $q$  to  $r_1$  and  $r_2$ . And it is interesting to see that both  $\alpha$  and  $q$  have very little response to  $r_3$ . This also can be seen from Fig. 4.23, i.e.,  $r_3$  has

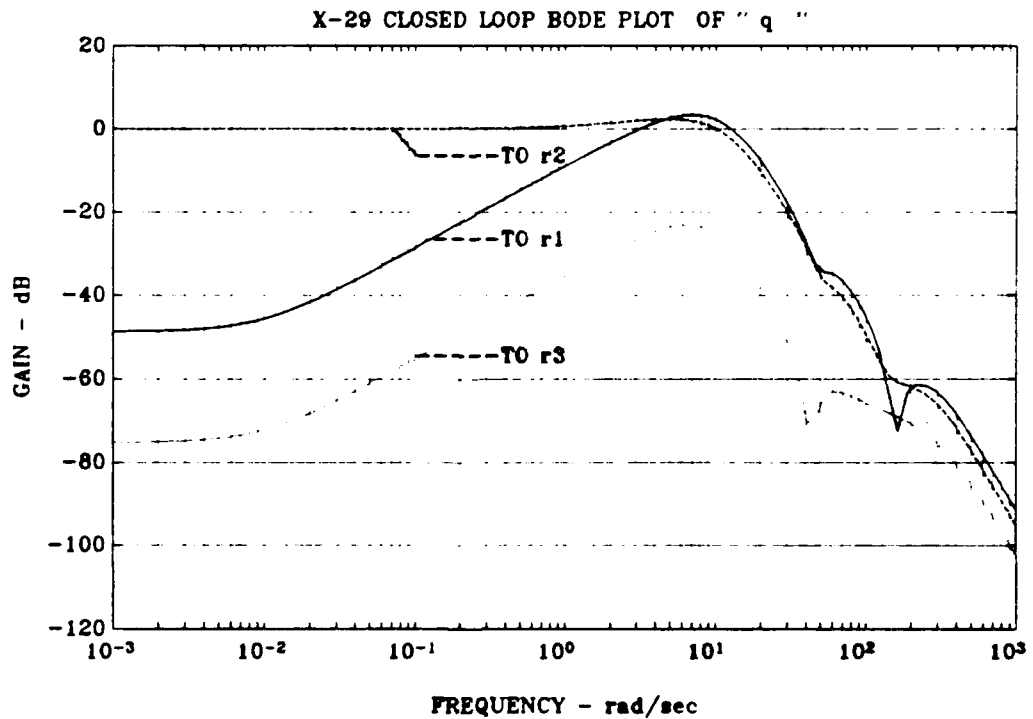
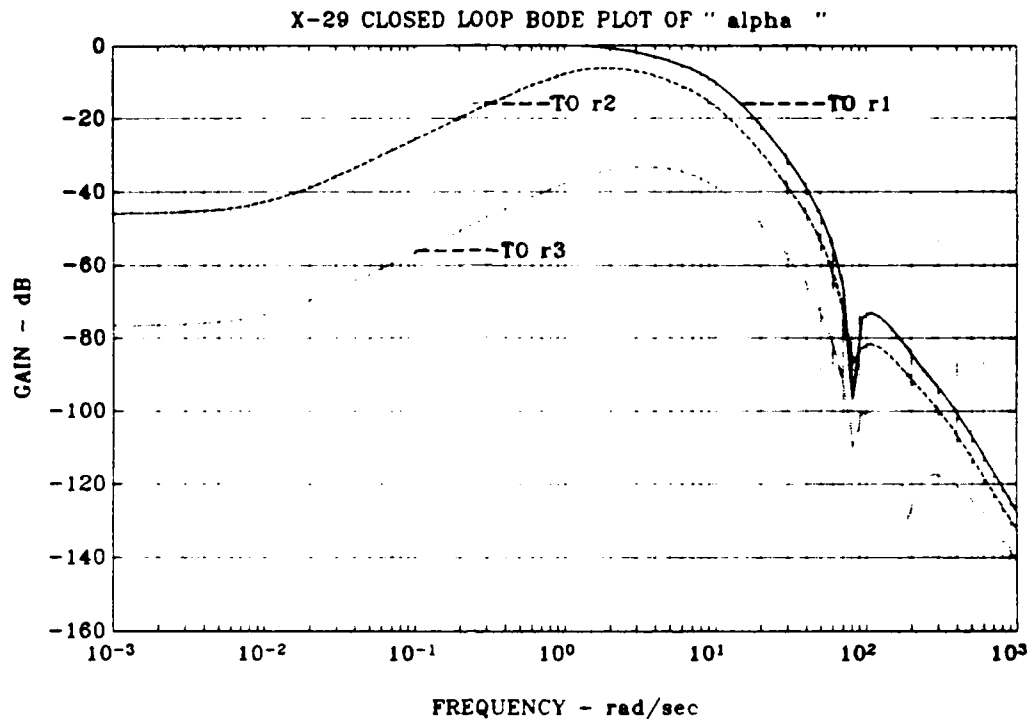


Figure 4.22 Closed Loop Bode Plots of  $\alpha$  and  $q$  for 3 I/O System

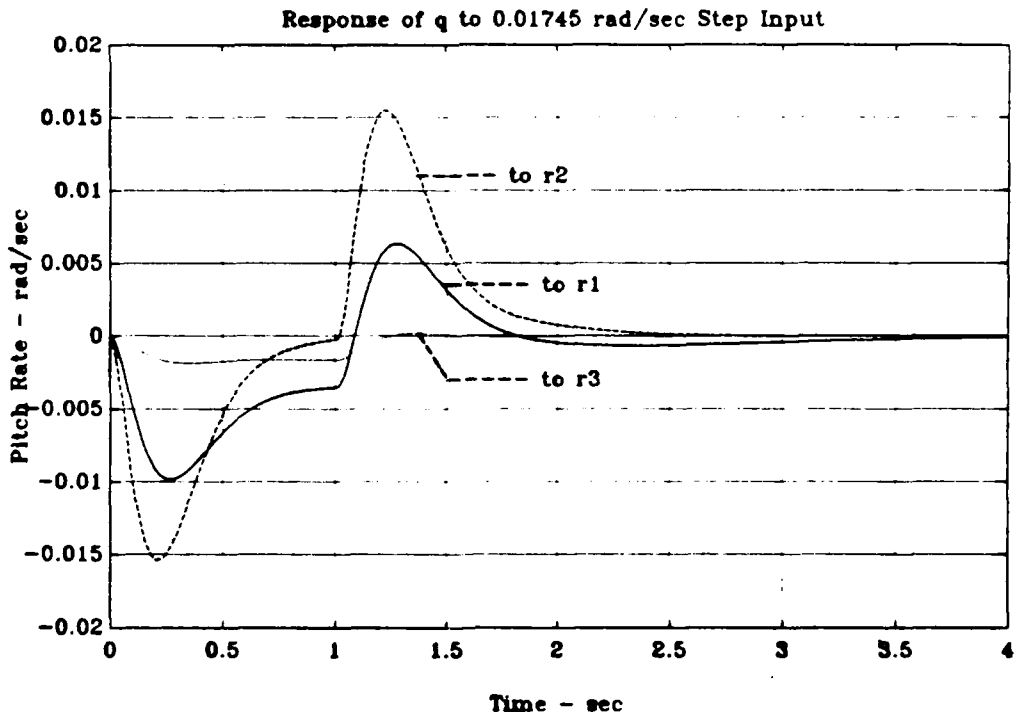
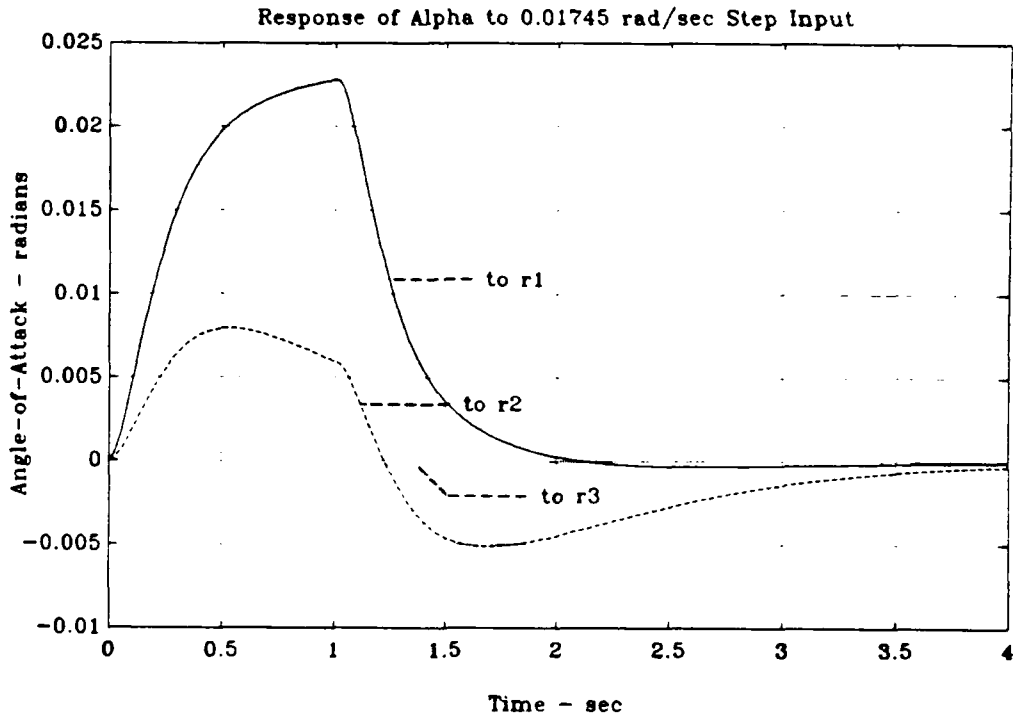


Figure 4.23 Step Response of  $\alpha$  and  $q$  for 3 I/O System

almost no effect on both  $\alpha$  and  $q$ . This indicates that there is not much difference to system response between 2 inputs design or 3 inputs design.

Shown in Fig. 4.24 and 4.25, the peak values of control deflections  $\delta_e$ ,  $\delta_r$ , and  $\delta_i$  (i.e., 0.005 rad, 0.0017 rad, and 0.015 rad respectively) are all well within the design limits listed before, and are also smaller than those of the 2 I/O system since the loop gains are smaller. Similar results are obtained from the plots of control rates (Fig. 4.26 and 4.27), i.e., all responses stay within their design limits.

Thus, we may conclude that the performance of this 3 I/O control system satisfies the design specifications but is not better than those of 2 I/O system designed previously.

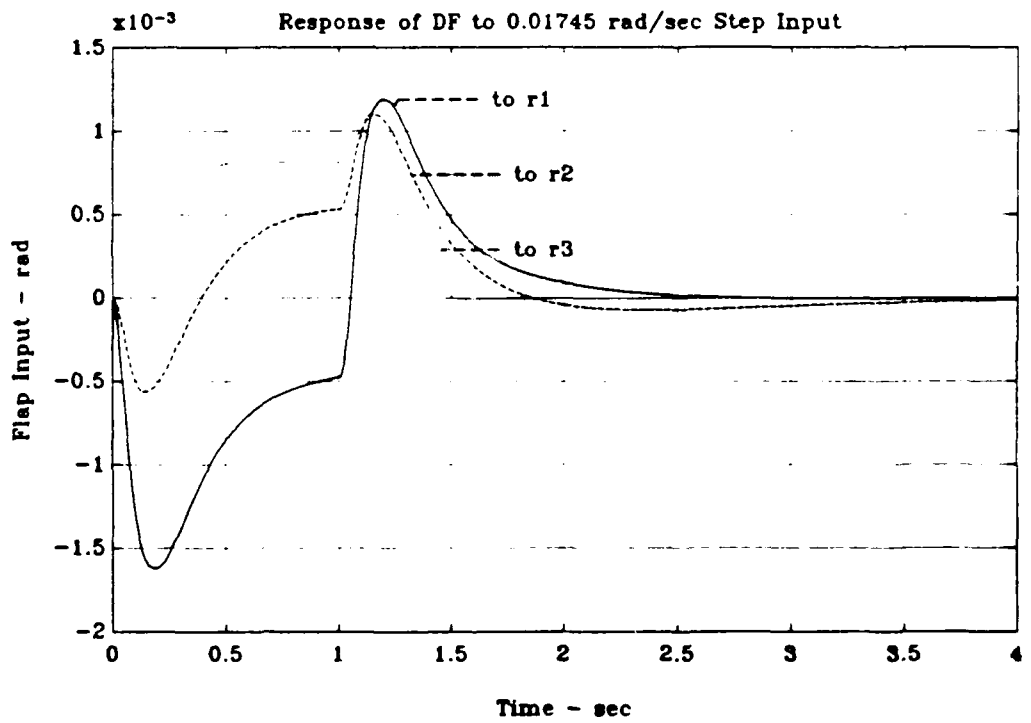
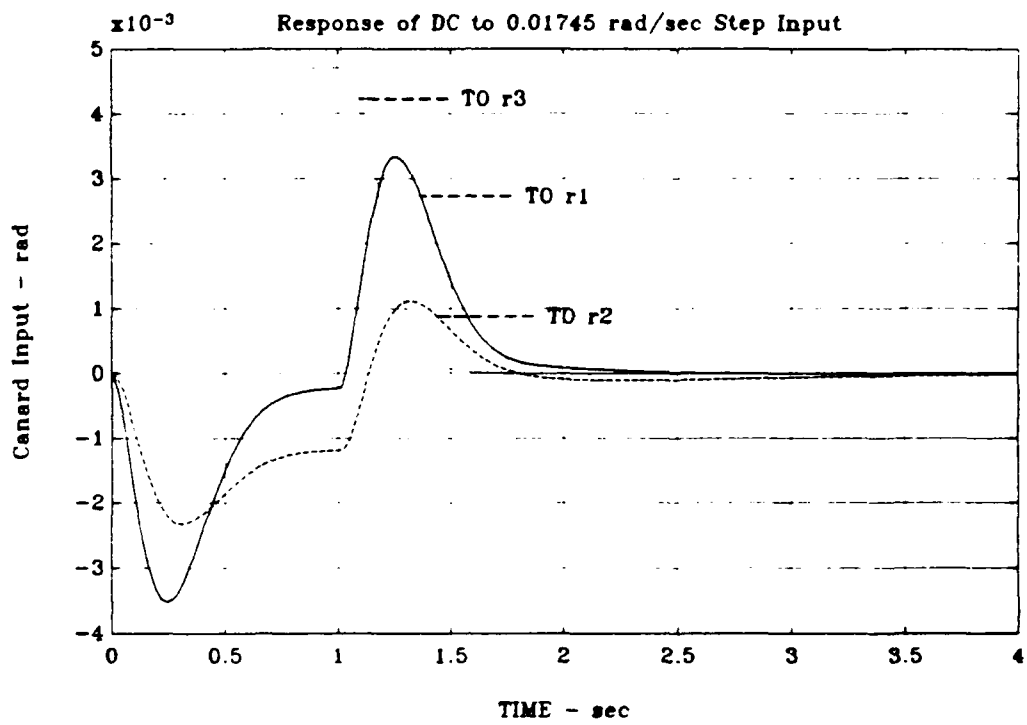


Figure 4.24 Step Response of  $\delta_c$  and  $\delta_f$  for 3 I/O System

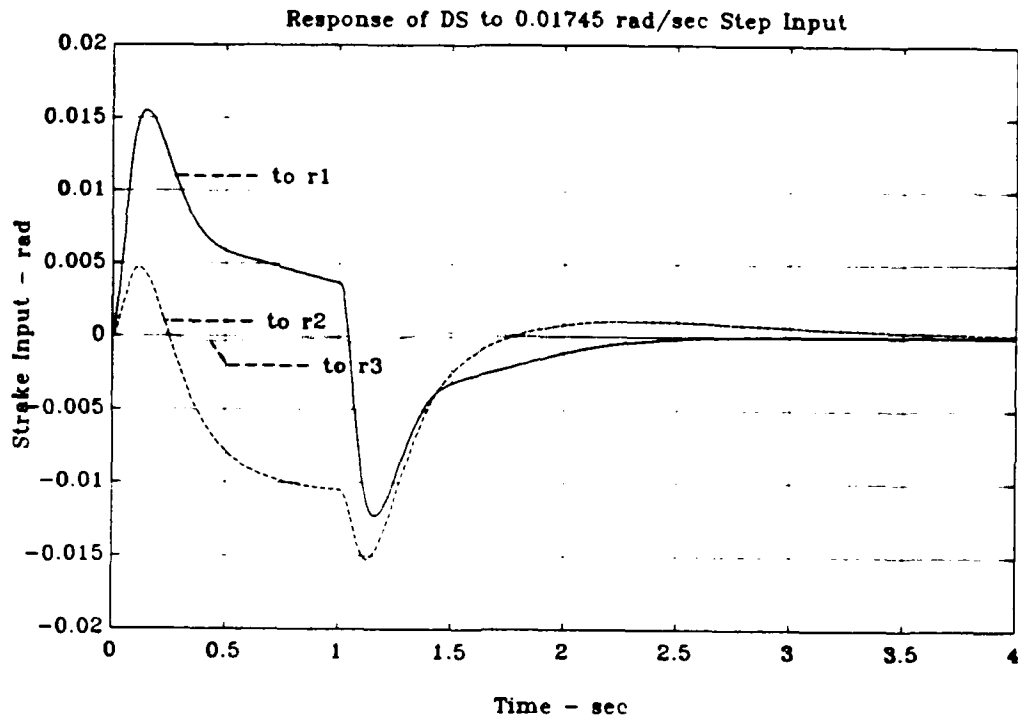


Figure 4.25 Step Response of  $\delta_c$  for 3 I/O System

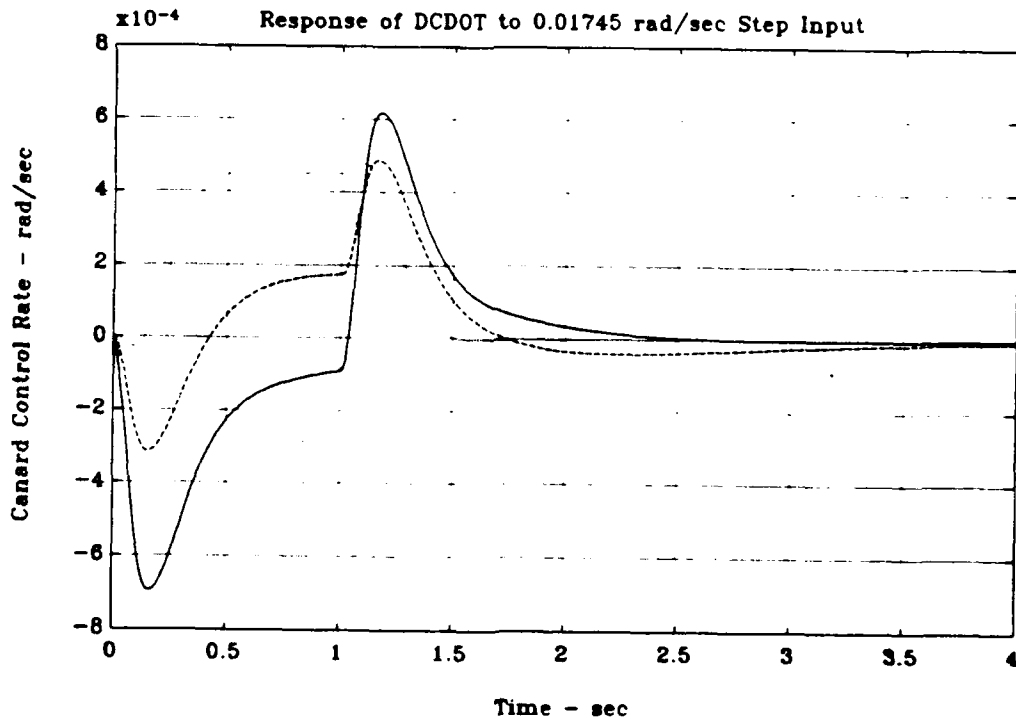


Figure 4.26 Step Response of  $\dot{\delta}_c$  for 3 I/O System

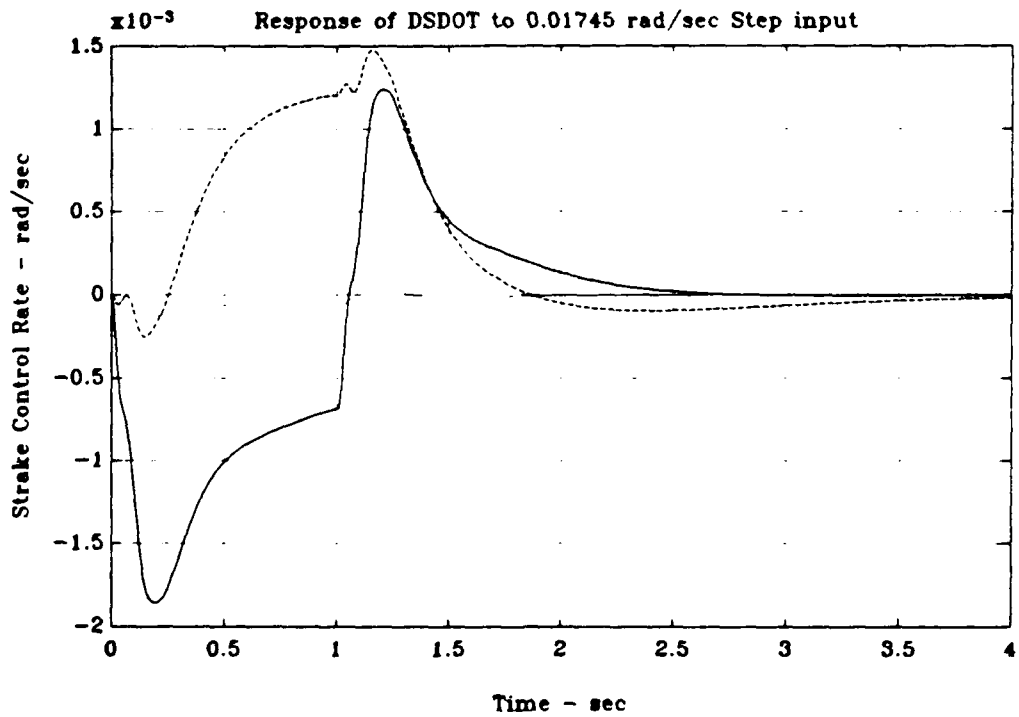
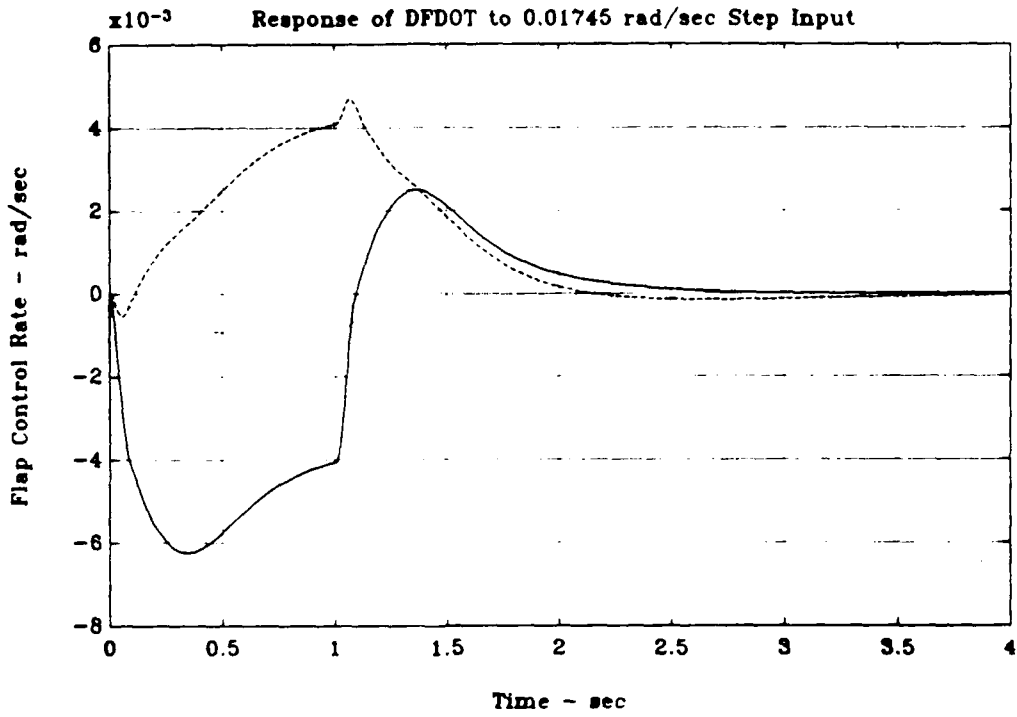


Figure 4.27 Step Response of  $\dot{\delta}_f$  and  $\dot{\delta}_s$  for 3 I/O System

## V. CONCLUSIONS AND RECOMMENDATIONS

Although the mathematic work behind the  $H_\infty$  theory is very complicated, the implementation of this method is easy using a well developed computer-aided design software. From the design procedure presented above, it is seen that  $H_\infty$  method provides a direct, systematic and effective way to synthesize controllers for the statically unstable longitudinal dynamics of X-29 aircraft. The two-command control design example demonstrates a fast response, large stability margins, good disturbance attenuation and low sensitivity performance. While the 3-input control configuration shows a somewhat less performance due to the smaller loop gains.

It is seen in both design cases that the two control outputs, angle-of-attack  $\alpha$  and pitch rate  $q$ , are decoupled to the command inputs. This is an important feature which is needed to effect the advanced control modes in which aircraft flight path and pitch attitude are independently controlled. Since, as shown in the 3-input case, the separated commanded strake has almost no influence on the control outputs, we may conclude that a reasonable and effective controller can be based on the use of two-command control in the X-29 control system .

In both designs, we found the peak values of control surface deflections for the actuators and control rates are all much smaller than their design limits. The selected  $W_2$  weighting matrix ensures this compatibility but at a severe penalty in performance.

Further reduced order modeling of the controller is possible but was not accomplished in this thesis.



```
cg=[1.0 0.0 0.0 0.0 0.0 0.0 0.0 0.0 0.0 0.0 0.0 0.0 0.0 0.0;
    0.0 1.0 0.0 0.0 0.0 0.0 0.0 0.0 0.0 0.0 0.0 0.0 0.0 0.0]
```

```
dg=zeros(2)
%pause
disp(' ')
disp(' Balanced realization of the X-29 state space representation')
disp(' ')
[agbl,bgbl,cgbl,g,t]=obalreal(ag,bg,cg)
ag=agbl; bg=bgbl; cg=cgbl;
%pause
w=logspace(-3,3,100);
svg=sigma(ag,bg,cg,dg,1,w); svg=20*log10(svg);
semilogx(w,svg)
title('X-29 SV PLOT OF PLANT G')
xlabel('FREQUENCY - rad/sec')
ylabel('SV - dB')
grid
meta hx29gsv
disp(' ')
disp(' Calculate the poles and transmission zeros of the balanced open')
disp(' loop plant')
disp(' ')
poleg=eig(ag), tzerog=tzero(ag,bg,cg,dg)
disp(' ')
disp(' ')
disp(' Determine determine the condition number of ag')
disp(' ')
disp(' ')
condag=cond(ag), rcondag=rcond(ag)
disp(' ')
disp(' ')
%pause
disp(' ')
disp(' << Design Specifications >> ')
disp(' ')
disp(' 1). Robustness Spec. : -40 dB roll-off, -20 db @ 100 Rad/Sec.')
disp(' Associated Weighting:')
disp(' ')
disp(' -1 1000 ')
disp(' W3(s) = ----- * I (fixd)')
disp(' 2 2x2')
disp(' s ')
disp(' ')
disp(' ')
disp(' 2). Performance Spec.: minimizing the sensitivity function')
disp(' as much as possible.')
disp(' Associated Weighting:')
disp(' ')
disp(' ')
disp(' -1 -1 .01(100s + 1) ')
disp(' W1(s) = Gam * ----- * I')
disp(' (.1s + 1) 2x2')
disp(' ')
disp(' where "Gam" in this design is iteratively updated from 1')
w=logspace(-3,3,100);
k=1000; mn=[2 2]; tau=0.0;
nuw3i = [0.0 k]; dnw3i = [1.0 0 0];
```

```

svw3i = bode(nuw3i,dnw3i,w); svw3i = 20*log10(svw3i);
nuw1i = [1.0 0.01]; dnw1i =[0.1 1.0];
svw1i = bode(nuw1i,dnw1i,w); svw1i = 20*log10(svw1i);
aw2=-0.025*eye(2); bw2=zeros(2); cw2=zeros(2); dw2=-0.025*eye(2);
disp(' ')
disp(' ')
disp('          (strike a key to see the plot of the weightings ...)')
%pause
semilogx(w,svw1i,w,svw3i)
grid
title('X-29 Design Specifications')
xlabel('Frequency - rad/sec')
ylabel('1/W1 & 1/W3 - db')
text(.01,0,'1/W1(s)')
text(.5,100,'1/W3(s)')
meta hx29specs
%pause
clc
disp('          << Problem Formulation >>')
disp(' ')
disp(' Form an augmented plant P(s) with these two weighting functions:')
disp(' ')
disp('          1). Gam*W1 penalizing error signal "e"')
disp(' ')
disp('          2). W3 penalizing plant output "y"')
disp(' ')
disp(' and find a stabilizing controller F(s) such that the Hinf norm')
disp(' of TF Tylul is less than or equal to one, i.e.')
disp(' ')
disp('          |Tylul| < or = 1,')
disp('          F(s) inf')
disp(' ')
disp(' where ')
disp('          Tylul =  $\begin{vmatrix} & -1 \\ \text{Gam} * \text{W1} * (\text{I} + \text{GF}) & \\ & -1 \\ \text{W3} * \text{GF} * (\text{I} + \text{GF}) & \end{vmatrix}$  =  $\begin{vmatrix} \text{Gam} * \text{W1} * \text{S} \\ \text{W3} * (\text{I} - \text{S}) \end{vmatrix}$  ')
disp(' ')
disp(' ')
disp('          (strike a key to continue ...)')
%pause
clc
disp(' ')
disp(' ')
disp('          << DESIGN PROCEDURE >>')
disp(' ')
disp(' *****')
disp(' * [Step 1]. Do plant augmentation (run AUGMENT.M or *')
disp(' * AUGX29.M) *')
disp(' * *')
disp(' * [Step 2]. Balance the augmented plant for better *')
disp(' * numerical condition if necessary *')
disp(' * *')
disp(' * [Step 3]. Do Hinf synthesis with "Gam" = 1 *')
disp(' * *')
disp(' * [Step 4]. Redo the plant augmentation for a *')
disp(' * higher "Gam" and rerun HINF.M *')
disp(' * *****')
disp(' ')

```

```

disp(' ')
disp('                                     (strike a key to continue ...)' )
%pause
clc
disp(' ')
disp(' ')
disp(' ')
disp(' Assign the cost coefficients "Gam" with Gam=1 ')
disp(' ')
disp(' serving as the baseline design ....' )
disp(' ')
disp(' -----')
disp(' augment      % Plant augmentation of the X-29 dynamics')
disp(' -----')
disp(' ')
disp(' ')
haugx29
disp(' ')
disp(' ')
disp('                                     (strike a key to continue ...)' )
%pause
clc
disp(' ')
disp(' ')
%disp(' Do state space balancing on the augmented plant if needed')
%disp(' ')
%disp(' ')
%[abal,bbal,cbal,g,t]=obalreal(A,[B1 B2],[C1;C2])
%A=abal, B1=bbal(:,1:2), B2=bbal(:,3:4), C1=cbal(1:4,:), C2=cbal(5:6,:)
disp(' ')
disp(' ')
disp(' The transmission zeros, poles and condition number of the augmented')
disp(' plant follow. In addition, determine if (A,B1) & (A,B2) are ')
disp(' stabilizable and if (C1,A) & (C2,A) are detectable.')
disp(' ')
disp(' ')
tzeroaug=tzero(A,[B1 B2],[C1;C2],[D11 D12;D21 D22]), poleaugA=eig(A)
condaugA=cond(A), rcondaugA=rcond(A)
eps=eps
toldef=10*max(size(A))*norm(A,1)*eps
tol=100*eps*norm([A B1])
[A1c,B1c,C1c,t,k]=ctrbf(A,B1,C1,tol)
tol=100*eps*norm([A B2])
[A2c,B2c,C2c,t,k]=ctrbf(A,B2,C2,tol)
tol=100*eps*norm([A;C1])
[A1o,B1o,C1o,t,k]=obsvf(A,B1,C1,tol)
tol=100*eps*norm([A;C2])
[A2o,B2o,C2o,t,k]=obsvf(A,B2,C2,tol)
clear condag rcondag poleg tzerog svw3i svwli
clear condauGA rcondaugA
clear functions
%pause
disp(' ')
disp(' ')
disp(' -----')
disp(' hinf      % Running script file HINF.M for Hinf optimization')
disp(' -----')
aretype='Schur'
hinf
disp(' ')

```

```

disp(' ')
disp('                                     (strike a key to continue ...)')
clear functions
%pause
disp(' ')
disp(' ')
disp('      State space representation of the full order controller')
disp('      (acp, bcp, ccp, dcp) with its poles and condition number')
disp(' ')
acp,bcp,ccp,dcp
polec=eig(acp)
condacp=cond(acp)
disp(' ')
disp('      Minimal realization of the controller')
disp(' ')
toldef=10*max(size(acp))*norm(acp,1)*eps
tol=100*eps*norm([acp bcp;ccp dcp])
[acpm,bcpm,ccpm,dcpm]=minreal(acp,bcp,ccp,dcp)
disp(' ')
disp('      Balanced realization & model reduction of the minimal controller')
disp(' ')
[acpbl,bcpbl,ccpbl,g,t]=obalreal(acpm,bcpm,ccpm)
elim=[10]
[acpr,bcpr,ccpr,dcpr]=modred(acpbl,bcpbl,ccpbl,dcpm,elim)
disp(' ')
disp('      Poles, controllability, observability, and condition of the ')
disp('      balanced, reduced order controller')
disp(' ')
poleacpr=eig(acpr)
tol=100*eps*norm([acpr bcpr])
[acpc,bcpc,ccpc,t,k]=ctrbf(acpr,bcpr,ccpr,tol)
tol=100*eps*norm([acpr;ccpr])
[acpo,bcpo,ccpo,t,k]=obsvf(acpr,bcpr,ccpr,tol)
condacpr=cond(acpr), rcondacpr=rcond(acpr)
acp=acpr; bcp=bcpr; ccp=ccpr; dcp=dcpr;
disp(' ')
disp('      CLTF Tylul (acl, bcl, ccl, dcl) and its poles (reduced order)')
[acl,bcl,ccl,dcl]=lftf(sysp,dimp,acp,bcp,ccp,dcp)
polet=eig(acl)
%pause
disp(' ')
disp(' ')
hplotmod          % Preparing singular values for plotting
end
disp(' ')
disp(' ')
disp('                                     (strike a key to continue ...)')
%pause
disp(' ')
disp(' ')
disp('      Open loop state space representation of controller/plant series')
disp(' ')
[algf,blgf,clgf,dlgf]=series(acp,bcp,ccp,dcp,ag,bg,cg,dg)
polol=eig(algf)
disp(' ')
disp(' ')
disp('                                     (strike a key to continue ...)')
%pause
disp(' ')
disp(' ')

```



```
cg=[1.0 0.0 0.0 0.0 0.0 0.0 0.0 0.0 0.0 0.0 0.0 0.0 0.0 0.0;
    0.0 1.0 0.0 0.0 0.0 0.0 0.0 0.0 0.0 0.0 0.0 0.0 0.0 0.0;
    0.0 0.0 1.0 0.0 0.0 0.0 0.0 0.0 0.0 0.0 0.0 0.0 0.0 0.0];
```

```
dg=zeros(3,3);
```

```
%pause
disp(' ')
disp('      Balanced realization of the X-29 state space representation')
disp(' ')
[agbl,bgbl,cgbl,g,t]=obalreal(ag,bg,cg)
ag=agbl,bg=bgbl,cg=cgbl,
w=logspace(-3,3,100);
svg=sigma(ag,bg,cg,dg,1,w);  svg=20*log10(svg);
semilogx(w,svg)
title('X-29 SV PLOT OF PLANT G')
xlabel('FREQUENCY - rad/sec')
ylabel('SV - dB')
grid
%meta h3x29gsv
disp(' ')
disp('      Calculate the poles and transmission zeros of the balanced open')
disp('      loop plant')
disp(' ')
poleg=eig(ag),  tzerog=tzero(ag,bg,cg,dg)
disp(' ')
disp(' ')
disp('      Determine determine the condition number of ag')
disp(' ')
disp(' ')
condag=cond(ag),  rcondag=rcond(ag)
disp(' ')
disp(' ')
%pause
disp(' ')
disp('      << Design Specifications >> ')
disp(' ')
disp('      1). Robustness Spec. : -40 dB roll-off, -20 db @ 100 Rad/Sec.')
disp('      Associated Weighting:')
disp(' ')
disp('      -1      1000 ')
disp('      W3(s) = ----- * I      (fixd)')
disp('              2      3x3')
disp('              s      ')
disp(' ')
disp(' ')
disp('      2). Performance Spec.: minimizing the sensitivity function')
disp('      as much as possible.')
disp('      Associated Weighting:')
disp(' ')
disp(' ')
disp('      -1      -1 .01(100s + 1) ')
disp('      W1(s) = Gam * ----- * I')
disp('              (.1s + 1)      ...3')
disp(' ')
disp(' ')
disp('      where "Gam" in this design is iteratively updated from 1')
w=logspace(-3,3,100);
```



```

disp(' ')
disp(' ')
disp(' ')
disp(' Assign the cost coefficients "Gam" with Gam=1 ')
disp(' ')
disp(' serving as the baseline design ....')
disp(' ')
disp(' -----')
disp(' augment % Plant augmentation of the X-29 dynamics')
disp(' -----')
disp(' ')
disp(' ')
h3augx29
disp(' ')
disp(' ')
disp(' (strike a key to continue ...)')
%pause
clc
disp(' ')
disp(' ')
%disp(' Do state space balancing on the augmented plant if needed')
%disp(' ')
%disp(' ')
%[abal,bbal,cbal,g,t]=obalreal(A,[B1 B2],[C1;C2])
%A=abal, B1=bbal(:,1:2), B2=bbal(:,3:4), C1=cbal(1:4,:), C2=cbal(5:6,:)
disp(' ')
disp(' ')
disp(' The transmission zeros, poles and condition number of the augmented')
disp(' plant follow. In addition, determine if (A,B1) & (A,B2) are ')
disp(' stabilizable and if (C1,A) & (C2,A) are detectable.')
disp(' ')
disp(' ')
tzeroaug=tzero(A,[B1 B2],[C1;C2],[D11 D12;D21 D22]), poleaugA=eig(A)
condaugA=cond(A), rcondaugA=rcond(A)
eps=eps
toldef=10*max(size(A))*norm(A,1)*eps
tol=100*eps*norm([A B1])
[A1c,B1c,C1c,t,k]=ctrbf(A,B1,C1,tol)
tol=100*eps*norm([A B2])
[A2c,B2c,C2c,t,k]=ctrbf(A,B2,C2,tol)
tol=100*eps*norm([A;C1])
[A1o,B1o,C1o,t,k]=obsvf(A,B1,C1,tol)
tol=100*eps*norm([A;C2])
[A2o,B2o,C2o,t,k]=obsvf(A,B2,C2,tol)
clear condag rcondag poleg tzerog svw3i svw1i
clear condaugA rcondaugA
clear functions
%pause
disp(' ')
disp(' ')
disp(' -----')
disp(' hinf % Running script file HINF.M for Hinf optimization')
disp(' -----')
aretype='Schur'
hinf
disp(' ')
disp(' ')
disp(' (strike a key to continue ...)')
clear functions
%pause

```

```

disp(' ')
disp(' ')
disp(' State space representation of the full order controller')
disp(' (acp, bcp, ccp, dcp) with its poles and condition number')
disp(' ')
acp,bcp,ccp,dcp
polec=eig(acp)
condacp=cond(acp)
disp(' ')
disp(' Minimal realization of the controller')
disp(' ')
toldef=10*max(size(acp))*norm(acp,1)*eps
tol=100*eps*norm([acp bcp;ccp dcp])
[acpm,bcpm,ccpm,dcpm]=minreal(acp,bcp,ccp,dcp)
disp(' ')
disp(' Balanced realization & model reduction of the minimal controller')
disp(' ')
[acpbl,bcpbl,ccpbl,g,t]=obalreal(acpm,bcpm,ccpm)
elim=[10]
[acpr,bcpr,ccpr,dcpr]=modred(acpbl,bcpbl,ccpbl,dcpm,elim)
disp(' ')
disp(' Poles, controllability, observability, and condition of the ')
disp(' balanced, reduced order controller')
disp(' ')
poleacpr=eig(acpr)
tol=100*eps*norm([acpr bcpr])
[acpc,bcpc,ccpc,t,k]=ctrbf(acpr,bcpr,ccpr,tol)
tol=100*eps*norm([acpr;ccpr])
[acpo,bcpo,ccpo,t,k]=obsvf(acpr,bcpr,ccpr,tol)
condacpr=cond(acpr), rcondacpr=rcond(acpr)
acp=acpr; bcp=bcpr; ccp=ccpr; dcp=dcpr;
disp(' ')
disp(' CLTF Tylul (acl, bcl, ccl, dcl) and its poles (reduced order)')
[acl,bcl,ccl,dcl]=lftf(syssp,dimp,acp,bcp,ccp,dcp)
polet=eig(acl)
%pause
disp(' ')
disp(' ')
h3plot % Preparing singular values for plotting
end
disp(' ')
disp(' ')
disp(' (strike a key to continue ...)')
%pause
disp(' ')
disp(' ')
disp(' Open loop state space representation of controller/plant series')
disp(' ')
[algf,blgf,clgf,dlgf]=series(acp,bcp,ccp,dcp,ag,bg,cg,dg)
polol=eig(algf)
disp(' ')
disp(' ')
disp(' (strike a key to continue ...)')
%pause
disp(' ')
disp(' ')
disp(' Closed loop state space representation of controller/plant series,')
disp(' controllability, observability, and condition number of the closed')
disp(' loop acgf matrix. ')
disp(' ')

```

```

disp(' ')
[acgf,bcgf,ccgf,dcgf]=feedbk(algf,blgf,clgf,dlgf,2)
tol=100*eps*norm([acgf bcgf])
[acgfc,bcgfc,ccgfc,t,k]=ctrbf(acgf,bcgf,ccgf,tol)
tol=100*eps*norm([acgf;ccgf])
[acgfo,bcgfo,ccgfo,t,k]=obsvf(acgf,bcgf,ccgf,tol)
condacgf=cond(acgf)
disp(' ')
disp(' ')
disp(' (strike a key to continue ...)')
%pause
disp(' ')
disp(' Poles of the closed loop system')
disp(' ')
polcl=eig(acgf)
h3aly
%h3rsp
end

```

```

%
% Plant Augmentation for the X-29 Hinf problem as W3 is not a
% proper transfer function. Includes contingency for adding W2 to
% ensure d12 is full column rank. This script file is designed for
% the X-29 system without theta as a state, ie, 3 inputs & 3 outputs.
%disp(' ')
%disp(' ')
%disp('          << Plant Augmentation >>')
%Gam=gama(1,i)
Gam = input('          Input the cost coefficient "Gam" = ')
cgb = 1/k*[cg(1,:)*ag*ag;
           cg(2,:)*ag*ag*ag*tau+cg(2,:)*ag*ag;
           cg(3,:)*ag*ag*ag*tau+cg(3,:)*ag*ag];
dgb = 1/k*[cg(1,:)*ag*bg;
           cg(2,:)*ag*ag*bg*tau;
           cg(3,:)*ag*ag*bg*tau];
nw1 = Gam*[dnw1i;0 0;0 0;0 0;dnw1i;0 0;0 0;0 0;dnw1i];
dw1 = nuw1i;
sysw2=[aw2 bw2;cw2 dw2]; xw2=3;
%[A,B1,B2,C1,C2,D11,D12,D21,D22]=haugmod(ag,bg,cg,cgb,dg,dgb,nw1,dw1,mn)
[A,B1,B2,C1,C2,D11,D12,D21,D22]=haugx29pl(ag,bg,cg,cgb,dg,dgb,nw1,dw1,sysw2,xw2,
%disp(' ')
%disp('          - - - State-Space (A,B1,B2,C1,C2,D11,D12,D21,D22) is ready for')
%disp('          the Small-Gain problem - - -')
%
% ----- End of AUGX29.M ----- % ^Z

```

```

disp('    Closed loop state space representation of controller/plant series,')
disp('    controllability, observability, and condition number of the closed')
disp('    loop acgf matrix. ')
disp(' ')
disp(' ')
[acgf,bcgf,ccgf,dcgf]=feedback(algf,blgf,clgf,dlgf,2)
tol=100*eps*norm([acgf bcgf])
[acgfc,bcgfc,ccgfc,t,k]=ctrbf(acgf,bcgf,ccgf,tol)
tol=100*eps*norm([acgf;ccgf])
[acgfo,bcgfo,ccgfo,t,k]=obsvf(acgf,bcgf,ccgf,tol)
condacgf=cond(acgf)
disp(' ')
disp(' ')
disp('                                (strike a key to continue ...)')
%pause
%diary hx29.dat
disp(' ')
disp('    Poles of the closed loop system')
disp(' ')
polcl=eig(acgf)
%h,29aly
%h,29trsp
enc

```

```

format short e
w=logspace(-3,3,100);
[mag1,phase1]=bode(algf,blgf,clgf,dlgf,1,w); mag1=20*log10(mag1);
[mag2,phase2]=bode(algf,blgf,clgf,dlgf,2,w); mag2=20*log10(mag2);
[mag3,phase3]=bode(algf,blgf,clgf,dlgf,3,w); mag3=20*log10(mag3);
semilogx(w,mag1(:,1),w,mag2(:,1),w,mag3(:,1))
title('X-29 OPEN LOOP (GF) BODE PLOT OF " alpha " ')
xlabel('FREQUENCY - rad/sec')
ylabel('GAIN - dB')
grid
%meta h3bd1
%pause
semilogx(w,mag1(:,2),w,mag2(:,2),w,mag3(:,2))
title('X-29 OPEN LOOP (GF) BODE PLOT OF " q " ')
xlabel('FREQUENCY - rad/sec')
ylabel('GAIN - dB')
grid
%meta h3bd2
%pause
[mag1,phase1]=bode(acgf,bcgf,ccgf,dcgf,1,w); mag1=20*log10(mag1);
[mag2,phase2]=bode(acgf,bcgf,ccgf,dcgf,2,w); mag2=20*log10(mag2);
[mag3,phase3]=bode(acgf,bcgf,ccgf,dcgf,3,w); mag3=20*log10(mag3);
semilogx(w,mag1(:,1),w,mag2(:,1),w,mag3(:,1))
title('X-29 CLOSED LOOP BODE PLOT OF " alpha " ')
xlabel('FREQUENCY - rad/sec')
ylabel('GAIN - dB')
grid
text(15,-20,'-----TO r1')
text(.22,-20,'-----TO r2')
text(.1,-60,'-----TO r3')
meta h3bd3
pause
semilogx(w,mag1(:,2),w,mag2(:,2),w,mag3(:,2))
title('X-29 CLOSED LOOP BODE PLOT OF " q " ')
xlabel('FREQUENCY - rad/sec')
ylabel('GAIN - dB')
grid
text(.1,-10,'-----TO r2')
text(.1,-30,'-----TO r1')
text(.1,-58,'-----TO r3')
meta h3bd4
%pause
disp(' ')
end

```

## APPENDIX B

### State Space Realization of the Open Loop Plant G

```
ag=[-.4181d+00 .9960d+00 -.2269d-01 -.1213d+00 -.1948d-01 -.9493d-03 ...  
.4427d-04 -.6712d-04 .1451d-05 -.2162d-04 -.3540d-05 0.0 0.0 0.0;  
.5474d+01 -.3424d+00 .2585d+01 -.1386d+01 -.1058d+01 .3898d-02 ...  
-.1164d-01 -.6397d-02 -.2509d-03 -.5367d-03 -.2912d-03 0.0 0.0 0.0;  
0.0 0.0 0.0 0.0 0.0 1.0 0.0 0.0 0.0 0.0 0.0 0.0 0.0 0.0;  
0.0 0.0 0.0 0.0 0.0 0.0 1.0 0.0 0.0 0.0 0.0 0.0 0.0 0.0;  
0.0 0.0 0.0 0.0 0.0 0.0 0.0 1.0 0.0 0.0 0.0 0.0 0.0 0.0;  
0.0 0.0 0.0 0.0 0.0 0.0 0.0 0.0 1.0 0.0 0.0 0.0 0.0 0.0;  
0.0 0.0 0.0 0.0 0.0 0.0 0.0 0.0 0.0 1.0 0.0 0.0 0.0 0.0;  
0.0 0.0 0.0 0.0 0.0 0.0 0.0 0.0 0.0 0.0 1.0e+04 0.0 0.0;  
0.0 0.0 0.0 0.0 0.0 0.0 0.0 0.0 0.0 0.0 0.0 1.0e+04 0.0;  
0.0 0.0 0.0 0.0 0.0 0.0 0.0 0.0 0.0 0.0 0.0 0.0 1.0e+04;  
0.0 0.0 -.1479d+04 0.0 0.0 -.1143d+03 0.0 0.0 -.2529d+01 0.0 ...  
0.0 -.2697d+03 0.0 0.0;  
0.0 0.0 0.0 -.1491d+04 0.0 0.0 -.1149d+03 0.0 0.0 -.2536d+01 ...  
0.0 0.0 -.2701d+03 0.0;  
0.0 0.0 0.0 0.0 -.5302d+05 0.0 0.0 -.1816d-04 0.0 0.0 ...  
-.1790d+02 0.0 0.0 -.6053d+03]
```

```
bg=[0.0 0.0;  
0.0 0.0;  
0.0 0.0;  
0.0 0.0;  
0.0 0.0;  
0.0 0.0;  
0.0 0.0;  
0.0 0.0;  
0.0 0.0;  
0.0 0.0;  
0.0 0.0;  
0.0 0.0;  
0.0 0.0;  
0.0 0.0;  
0.0 0.0;  
.1479d+04 0.0;  
0.0 .1491d+04;  
.5308d+05 0.0]
```

```
cg=[1.0 0.0 0.0 0.0 0.0 0.0 0.0 0.0 0.0 0.0 0.0 0.0 0.0 0.0;  
0.0 1.0 0.0 0.0 0.0 0.0 0.0 0.0 0.0 0.0 0.0 0.0 0.0 0.0]
```

```
dg=zeros(2)
```

## APPENDIX C

### State Space Realization of Reduced-Order Controller for 2 I/O System

acpr =

Columns 1 through 6

-1.0399e-02	-1.2262e-05	-1.0460e-01	4.8094e-02	-7.6875e-02	1.3274e-02
-1.1271e-04	-1.0156e-02	-4.6795e-03	8.3252e-02	-3.1861e-02	-2.8000e-02
-1.0340e-01	-2.9977e-02	-1.9525e+01	2.6394e+01	-3.1280e+01	4.9271e+00
-5.7615e-02	6.0104e-02	-2.7029e+01	-2.5674e+01	4.0396e+01	-7.7033e-02
7.8601e-02	1.3419e-02	3.1746e+01	3.6483e+01	-1.2030e+02	5.3509e+01
-3.4048e-03	-3.6138e-02	-2.7492e+00	5.9997e+00	-2.9572e+01	-9.8984e+00
-4.9864e-03	-3.9735e-02	-3.1302e+00	3.5764e+00	5.9253e+01	-2.4777e+01
3.6535e-03	-2.9112e-02	2.9037e-01	1.0513e+01	-2.4717e+01	-2.1685e+01
4.7908e-02	-1.1300e-02	1.7010e+01	3.2813e+01	-1.4766e+02	1.0290e+01
9.2037e-03	-1.4652e-03	3.2877e+00	6.3758e+00	-2.8661e+01	8.9049e-01
-8.7200e-04	6.8844e-03	-9.9621e-02	-2.1329e+00	1.6446e+00	3.5846e+00
8.3046e-04	-3.7921e-03	1.8196e-01	1.4002e+00	-1.9663e+00	-1.8969e+00
8.2445e-04	1.0942e-04	3.0302e-01	5.1368e-01	-2.5218e+00	1.7864e-01
-1.7763e-04	9.0089e-04	-3.6094e-02	-3.1981e-01	4.0668e-01	4.5402e-01
2.3188e-05	3.6527e-05	9.5788e-03	6.8832e-03	-7.5896e-02	2.2842e-02

Columns 7 through 12

2.5870e-03	9.1286e-03	8.3886e-03	8.6940e-03	5.3095e-04	1.7503e-03
-4.0336e-02	2.5238e-02	-8.4033e-02	-5.5085e-03	-7.0034e-03	-2.6531e-03
9.2118e-01	3.4965e+00	2.3161e+00	3.1564e+00	1.5463e-01	6.2854e-01
1.0142e+01	-1.3763e+01	1.9246e+01	-3.0766e+00	1.8510e+00	-1.3642e-01
-5.1779e+01	4.6467e+01	1.9853e+01	2.4744e+01	-1.1656e+00	4.1721e+00
3.2298e+00	1.4770e+01	-4.2332e+01	-7.6418e+00	-3.2832e+00	-2.1705e+00
-1.3998e+01	3.5254e+01	-6.3778e+01	-5.0628e+00	-4.9278e+00	-2.0558e+00
-3.7012e+01	-1.4396e+01	9.7679e+01	-3.0219e+00	5.0051e+00	5.6593e-01
2.0492e+01	-7.6498e+01	-2.4305e+02	-2.9439e+01	-4.1233e+01	-1.7944e+01
1.5648e+00	-4.6369e+00	-8.7073e+01	-4.5600e+01	-2.4619e+01	-2.1083e+01
4.4792e+00	6.6710e+00	1.6807e+01	2.0142e+01	-2.7237e+01	-2.5895e+01
-2.3356e+00	-3.8924e+00	-1.1275e+01	-9.7936e+00	3.2961e+01	-1.2550e+02
2.7969e-01	-2.1520e-01	-8.1078e+00	-8.0534e+00	1.9334e+00	-2.7568e+01
5.6035e-01	9.1670e-01	2.5024e+00	2.2396e+00	-7.3070e+00	5.7380e+01
3.0310e-02	2.5482e-02	-2.0105e-01	-2.0731e-01	-2.0302e-01	1.1700e+00

Columns 13 through 15

-4.8787e-04	-4.7600e-04	-1.1648e-05
-1.1798e-03	-4.6223e-04	-5.0636e-05
-1.8641e-01	-1.7785e-01	-4.5815e-03
6.2164e-01	3.9705e-01	2.1676e-02
-1.9086e+00	-1.5949e+00	-5.4329e-02
-1.9215e-01	9.8820e-02	-1.3922e-02
-7.3742e-01	-2.4886e-01	-3.2950e-02
1.4035e+00	8.0952e-01	5.1750e-02
-5.7313e+00	-1.7434e+00	-2.6308e-01
2.3404e+00	3.5305e+00	1.1476e-02
-8.1543e+00	-2.5954e+00	-3.6511e-01
2.4647e+00	1.5106e+01	-1.0758e+00
-4.5631e+01	-6.3440e+01	-3.3130e+00
3.3396e+01	-7.1315e+01	-6.2957e+00
-2.7014e+00	-3.0793e+00	-1.4418e+02

bcpr =

5.2502e+00	6.4618e-01
-3.2830e-01	2.9101e+00
2.5970e+01	7.3091e+00
1.5589e+01	-7.1255e+00
-1.9609e+01	-4.1407e+00
2.1893e-01	5.2816e+00
5.5783e-01	5.8452e+00
-1.4366e+00	4.0563e+00
-1.2310e+01	2.5979e-01
-2.3522e+00	-5.2653e-02
3.4165e-01	-9.6027e-01
-2.7670e-01	5.1899e-01
-2.0646e-01	-3.9167e-02
6.0765e-02	-1.2386e-01
-5.2177e-03	-5.8883e-03

ccpr =

Columns 1 through 6

-3.8779e+00	1.9829e+00	-1.9257e+01	7.1236e-01	-1.1251e+01	5.2413e+00
-3.5979e+00	-2.1551e+00	-1.8895e+01	1.7126e+01	-1.6585e+01	-6.8677e-01

Columns 7 through 12

4.4501e+00	-7.6160e-01	9.8134e+00	2.1675e+00	7.8612e-01	5.8776e-01
-3.8307e+00	4.2352e+00	-7.4360e+00	9.1514e-01	-6.4874e-01	2.1019e-02

Columns 13 through 15

2.4380e-02	-4.3767e-02	2.7852e-03
-2.0872e-01	-1.3083e-01	-7.3580e-03

dcpr =

-3.9822e-01	-9.2951e-02
-6.3988e-02	-1.4936e-02

## APPENDIX D

### Closed Loop State Space Realization of Controller/Plant Series

Columns 1 through 6

-1.0399e-02	-1.2262e-05	-1.0460e-01	4.8094e-02	-7.6875e-02	1.3274e-02
-1.1271e-04	-1.0156e-02	-4.6795e-03	8.3252e-02	-3.1861e-02	-2.8000e-02
-1.0340e-01	-2.9977e-02	-1.9525e+01	2.6394e+01	-3.1280e+01	4.9271e+00
-5.7615e-02	6.0104e-02	-2.7029e+01	-2.5674e+01	4.0396e+01	-7.7033e-02
7.8601e-02	1.3419e-02	3.1746e+01	3.6483e+01	-1.2030e+02	5.3509e+01
-3.4048e-03	-3.6138e-02	-2.7492e+00	5.9997e+00	-2.9572e+01	-9.8984e+00
-4.9864e-03	-3.9735e-02	-3.1302e+00	3.5764e+00	5.9253e+01	-2.4777e+01
3.6535e-03	-2.9112e-02	2.9037e-01	1.0513e+01	-2.4717e+01	-2.1685e+01
4.7908e-02	-1.1300e-02	1.7010e+01	3.2813e+01	-1.4766e+02	1.0290e+01
9.2037e-03	-1.4652e-03	3.2877e+00	6.3758e+00	-2.8661e+01	8.9049e-01
-8.7200e-04	6.8844e-03	-9.9621e-02	-2.1329e+00	1.6446e+00	3.5846e+00
8.3046e-04	-3.7921e-03	1.8196e-01	1.4002e+00	-1.9663e+00	-1.8969e+00
8.2445e-04	1.0942e-04	3.0302e-01	5.1368e-01	-2.5218e+00	1.7864e-01
-1.7763e-04	9.0089e-04	-3.6094e-02	-3.1981e-01	4.0668e-01	4.5402e-01
2.3188e-05	3.6527e-05	9.5788e-03	6.8832e-03	-7.5896e-02	2.2842e-02
-1.2486e+00	-2.9277e-01	-6.4400e+00	4.0675e+00	-5.0553e+00	3.9391e-01
6.2283e-01	-3.5136e+00	2.2704e+00	1.3055e+01	-3.1083e+00	-5.2805e+00
-2.8230e+00	4.3606e+00	-1.3268e+01	-1.1504e+01	-3.7032e+00	7.8679e+00
4.5916e-01	-1.8217e+00	1.8716e+00	6.4561e+00	-1.1091e+00	-2.8251e+00
-2.6795e+00	7.0049e-01	-1.3478e+01	3.2523e+00	-8.8046e+00	2.6913e+00
3.3498e+00	-6.0600e-01	1.6920e+01	-5.1776e+00	1.1422e+01	-2.9899e+00
-1.1953e+00	1.4172e+00	-5.7285e+00	-3.1023e+00	-2.2283e+00	2.7353e+00
-1.9331e-01	9.0043e-01	-7.5360e-01	-3.2683e+00	6.7229e-01	1.3748e+00
1.1620e+00	-1.4093e-01	5.8870e+00	-2.0816e+00	4.0687e+00	-9.4087e-01
-9.4959e-01	5.5372e-01	-4.6981e+00	-1.0641e-01	-2.6504e+00	1.3781e+00
-4.6009e-01	1.0922e-02	-2.3425e+00	1.0092e+00	-1.6801e+00	3.1020e-01
1.4474e-01	7.9646e-02	7.5834e-01	-6.5991e-01	6.5636e-01	1.7830e-02
1.3788e-02	-9.7163e-02	4.5274e-02	3.6887e-01	-9.8623e-02	-1.4382e-01
1.3630e-02	-6.9743e-03	6.7686e-02	-2.4859e-03	3.9541e-02	-1.8429e-02

Columns 7 through 12

2.5870e-03	9.1286e-03	8.3886e-03	8.6940e-03	5.3095e-04	1.7503e-03
-4.0336e-02	2.5238e-02	-8.4033e-02	-5.5085e-03	-7.0034e-03	-2.6531e-03
9.2118e-01	3.4965e+00	2.3161e+00	3.1564e+00	1.5463e-01	6.2854e-01
1.0142e+01	-1.3763e+01	1.9246e+01	-3.0766e+00	1.8510e+00	-1.3642e-01
-5.1779e+01	4.6467e+01	1.9853e+01	2.4744e+01	-1.1656e+00	4.1721e+00
3.2298e+00	1.4770e+01	-4.2332e+01	-7.6418e+00	-3.2832e+00	-2.1705e+00
-1.3998e+01	3.5254e+01	-6.3778e+01	-5.0628e+00	-4.9278e+00	-2.0558e+00
-3.7012e+01	-1.4396e+01	9.7679e+01	-3.0219e+00	5.0051e+00	5.6593e-01
2.0492e+01	-7.6498e+01	-2.4305e+02	-2.9439e+01	-4.1233e+01	-1.7944e+01
1.5648e+00	-4.6369e+00	-8.7073e+01	-4.5600e+01	-2.4619e+01	-2.1083e+01
4.4792e+00	6.6710e+00	1.6807e+01	2.0142e+01	-2.7237e+01	-2.5895e+01
-2.3356e+00	-3.8924e+00	-1.1275e+01	-9.7936e+00	3.2961e+01	-1.2550e+02
2.7969e-01	-2.1520e-01	-8.1078e+00	-8.0534e+00	1.9334e+00	-2.7568e+01
5.6035e-01	9.1670e-01	2.5024e+00	2.2396e+00	-7.3070e+00	5.7380e+01
3.0310e-02	2.5482e-02	-2.0105e-01	-2.0731e-01	-2.0302e-01	1.1700e+00
-4.2260e-01	9.0677e-01	-6.9611e-01	4.4243e-01	-6.8136e-02	6.7025e-02
-7.0809e+00	4.0749e+00	-1.4806e+01	-1.2247e+00	-1.2285e+00	-5.1375e-01
9.0516e+00	-4.1630e+00	1.9222e+01	2.3782e+00	1.5786e+00	8.1073e-01
-3.6887e+00	2.0533e+00	-7.7326e+00	-6.9198e-01	-6.4051e-01	-2.7787e-01
1.7406e+00	3.0217e-01	4.0080e+00	1.3140e+00	3.1217e-01	3.1824e-01
-1.6387e+00	-7.1145e-01	-3.8938e+00	-1.5687e+00	-2.9721e-01	-3.6245e-01
2.9776e+00	-1.2318e+00	6.3622e+00	8.8925e-01	5.2036e-01	2.8696e-01
1.8190e+00	-1.0296e+00	3.8082e+00	3.2795e-01	3.1571e-01	1.3450e-01
-4.3037e-01	-3.3250e-01	-1.0638e+00	-5.2515e-01	-7.9197e-02	-1.1663e-01
1.2255e+00	-2.7079e-01	2.6852e+00	5.4947e-01	2.1601e-01	1.5287e-01
8.0992e-02	1.8717e-01	2.3541e-01	1.9563e-01	1.5877e-02	4.0291e-02
1.4006e-01	-1.6166e-01	2.6995e-01	-3.8751e-02	2.3666e-02	-1.7713e-03
-1.9537e-01	1.1418e-01	-4.0801e-01	-3.2428e-02	-3.3881e-02	-1.3917e-02
-1.5651e-02	2.6824e-03	-3.4512e-02	-7.6200e-03	-2.7647e-03	-2.0665e-03

## Columns 13 through 18

-4.8787e-04	-4.7600e-04	-1.1648e-05	3.4265e+00	2.6093e-01	7.0033e-01
-1.1798e-03	-4.6223e-04	-5.0636e-05	3.2032e-02	3.9424e+00	4.6163e+00
-1.8641e-01	-1.7785e-01	-4.5815e-03	1.7292e+01	6.8088e+00	9.9599e+00
6.2164e-01	3.9705e-01	2.1676e-02	9.4193e+00	-1.1360e+01	-1.2205e+01
-1.9086e+00	-1.5949e+00	-5.4329e-02	-1.2942e+01	-3.2921e+00	-5.3438e+00
-1.9215e-01	9.8820e-02	-1.3922e-02	5.8151e-01	7.0611e+00	8.3284e+00
-7.3742e-01	-2.4886e-01	-3.2950e-02	8.4625e-01	7.7782e+00	9.1980e+00
1.4035e+00	8.0952e-01	5.1750e-02	-5.8424e-01	5.6082e+00	6.4942e+00
-5.7313e+00	-1.7434e+00	-2.6308e-01	-7.8856e+00	1.7695e+00	1.1612e+00
2.3404e+00	3.5305e+00	1.1476e-02	-1.5154e+00	2.0088e-01	6.0322e-02
-8.1543e+00	-2.5954e+00	-3.6511e-01	1.3931e-01	-1.3278e+00	-1.5375e+00
2.4647e+00	1.5106e+01	-1.0758e+00	-1.3442e-01	7.2827e-01	8.3657e-01
-4.5631e+01	-6.3440e+01	-3.3130e+00	-1.3589e-01	-2.8718e-02	-4.9266e-02
3.3396e+01	-7.1315e+01	-6.2957e+00	2.8694e-02	-1.7319e-01	-1.9933e-01
-2.7014e+00	-3.0793e+00	-1.4418e+02	-3.8432e-03	-7.2981e-03	-8.9818e-03
-4.6078e-02	-3.5124e-02	-1.4208e-03	1.2250e-01	2.2308e+00	8.2904e-02
-1.8895e-01	-6.5135e-02	-8.3992e-03	2.5142e+00	-6.6192e-01	-1.7140e+00
1.8667e-01	3.4021e-02	9.2872e-03	1.0453e-01	1.5308e+00	-1.4431e+01
-9.4784e-02	-3.0659e-02	-4.2791e-03	1.4115e-01	-5.6614e-01	1.2023e+01
-2.1934e-02	-4.5366e-02	2.5787e-04	-2.7934e-01	2.0713e-01	-7.7357e+00
4.3042e-02	6.2808e-02	3.4892e-04	2.7402e-01	-2.0757e-01	7.7828e+00
5.4190e-02	4.7124e-03	2.8644e-03	-1.2447e-01	4.5133e-01	-9.8684e+00
4.7635e-02	1.5922e-02	2.1338e-03	-5.0931e-02	2.7919e-01	-5.4553e+00
1.8943e-02	2.3352e-02	2.9346e-04	8.3725e-02	-5.0725e-02	2.1914e+00
9.9162e-03	-9.1785e-03	8.5161e-04	-8.4322e-02	1.8042e-01	-4.3499e+00
-1.0099e-02	-1.0260e-02	-2.2788e-04	-3.6226e-02	5.8282e-03	-6.0937e-01
7.9885e-03	5.1041e-03	2.7846e-04	4.8150e-03	2.2795e-02	-2.9610e-01
-5.3051e-03	-1.8796e-03	-2.3417e-04	4.2518e-03	-3.0401e-02	5.8408e-01
-8.5947e-05	1.5374e-04	-9.8005e-06	2.9774e-04	-2.2133e-03	5.6798e-02

## Columns 19 through 24

-3.6426e-01	-2.1595e+00	2.4683e-01	-2.2989e-01	-2.2162e-01	1.8631e-03
1.8269e+00	-1.1359e+00	1.9499e+00	-1.5626e+00	8.9748e-01	-6.5908e-01
7.1306e-01	-1.2453e+01	3.9605e+00	-3.3354e+00	1.3545e-01	-9.0933e-01
-6.6120e+00	-2.5162e+00	-5.2915e+00	4.1514e+00	-3.3666e+00	2.0255e+00
3.0422e-01	8.8093e+00	-2.0725e+00	1.7819e+00	3.1041e-01	3.7883e-01
3.1979e+00	-2.3535e+00	3.5104e+00	-2.8181e+00	1.5644e+00	-1.1735e+00
3.4936e+00	-2.7178e+00	3.8740e+00	-3.1119e+00	1.7064e+00	-1.2899e+00
2.6881e+00	-1.2326e+00	2.7522e+00	-2.1996e+00	1.3284e+00	-9.4593e-01
1.9393e+00	4.2986e+00	6.0352e-01	-4.0962e-01	1.0512e+00	-4.0076e-01
3.0803e-01	8.6546e-01	4.7184e-02	-2.3598e-02	1.7023e-01	-5.3733e-02
-6.3660e-01	2.9124e-01	-6.5159e-01	5.2077e-01	-3.1460e-01	2.2398e-01
3.5737e-01	-1.2442e-01	3.5538e-01	-2.8348e-01	1.7731e-01	-1.2361e-01
5.9127e-03	9.0844e-02	-1.8869e-02	1.6393e-02	4.5954e-03	2.9990e-03
-8.4524e-02	3.1581e-02	-8.4626e-02	6.7536e-02	-4.1897e-02	2.9354e-02
-2.8459e-03	4.4059e-03	-3.7398e-03	3.0324e-03	-1.3509e-03	1.1698e-03
-3.1731e-02	-1.7755e-01	1.8591e-02	-1.7428e-02	-1.9176e-02	8.0964e-04
-6.6508e-01	2.8540e-01	-6.7816e-01	5.4144e-01	-3.3059e-01	2.3398e-01
-1.1960e+01	8.1671e+00	-1.2278e+01	9.8902e+00	5.4148e+00	4.0581e+00
-3.2752e+01	2.5403e+01	-6.5244e+01	4.3819e+01	-3.6204e+01	2.3589e+01
1.2476e+01	-3.3664e+01	3.1172e+01	-3.4986e+01	2.4951e+01	-1.9603e+01
-9.8155e+00	6.6774e+01	-1.1499e+02	2.3948e+02	-1.3531e+02	8.5371e+01
4.1919e+01	-3.7902e+01	-6.7843e+01	-9.1153e+01	1.7521e+02	-8.2929e+01
3.6204e+01	-2.3385e+01	9.0979e+01	-1.7323e+02	-7.3440e+01	1.0393e+02
-8.9347e+00	2.7218e+01	-8.5195e+01	5.6306e+01	6.6647e+00	-1.4028e+02
2.2762e+01	-3.0465e+01	8.6383e+01	-9.3371e+01	-8.1601e+01	1.3847e+02
1.7222e+00	-9.7024e+00	2.9393e+01	-1.4357e+01	-4.7599e+00	9.1385e+01
2.3936e+00	1.6034e+00	-6.0956e+00	-4.3450e+00	-1.1412e+01	-2.3750e+01
-3.4643e+00	1.9987e+00	-4.4409e+00	1.0620e+01	1.5786e+01	-1.2415e+01
-2.8422e-01	4.0575e-01	-1.1027e+00	1.1095e+00	1.2718e+00	-3.7835e+00

Columns 25 through 29

7.6382e-01	-1.6414e-01	-1.7640e-01	1.7079e-01	7.1694e-03
6.4187e-01	2.3732e-01	-5.7108e-02	2.4721e-02	-9.4652e-03
4.7395e+00	-4.9543e-01	-9.6751e-01	8.9417e-01	2.2894e-02
1.5408e-01	-1.1834e+00	-3.1491e-01	3.9862e-01	4.8928e-02
-3.2565e+00	4.8012e-01	6.9870e-01	-6.5861e-01	-2.1497e-02
1.2600e+00	3.9753e-01	-1.2870e-01	7.0169e-02	-1.5760e-02
1.4313e+00	4.2710e-01	-1.5214e-01	8.7456e-02	-1.6892e-02
7.8041e-01	3.7067e-01	-4.9491e-02	4.0556e-03	-1.4898e-02
-1.3760e+00	5.2144e-01	3.7259e-01	-3.7915e-01	-2.2233e-02
-2.8685e-01	9.1768e-02	7.3560e-02	-7.3678e-02	-3.9359e-03
-1.8457e-01	-8.7815e-02	1.1669e-02	-9.1201e-04	3.5297e-03
8.9010e-02	5.1210e-02	-3.4755e-03	-2.3655e-03	-2.0680e-03
-3.3252e-02	5.3962e-03	7.2542e-03	-6.8813e-03	-2.3989e-04
-2.1857e-02	-1.2007e-02	9.9145e-04	4.0093e-04	4.8434e-04
-1.9853e-03	-2.4059e-04	2.9646e-04	-2.3268e-04	8.9075e-06
6.2396e-02	-1.3781e-02	-1.4500e-02	1.4070e-02	6.0100e-04
-1.8649e-01	-9.3084e-02	1.0728e-02	4.6116e-04	3.7462e-03
-4.2170e+00	-1.4053e+00	4.1395e-01	-2.1229e-01	5.5841e-02
-2.1484e+01	-8.7977e+00	1.5914e+00	-4.6398e-01	3.5200e-01
3.1664e+01	4.0658e+00	-4.5088e+00	3.4961e+00	-1.4919e-01
-8.5469e+01	-2.7750e+01	7.4458e+00	-3.5528e+00	1.0843e+00
8.7428e+01	2.7088e+01	-7.3769e+00	3.6175e+00	-1.0655e+00
-7.3125e+01	-3.9971e+01	7.1874e+00	-1.8422e+00	1.6118e+00
1.4883e+02	8.4695e+01	-2.1423e+01	1.0333e+01	-4.0479e+00
-2.1400e+02	-6.4387e+01	5.7274e+01	-4.1414e+01	3.2024e+00
-8.9390e+01	-1.1436e+02	-3.1523e+01	9.1100e+00	9.2255e+00
-8.0190e+00	8.5858e+01	-4.0464e+01	6.0359e+01	-9.2992e-01
4.3488e+01	9.8215e+00	3.1925e+01	-1.3722e+02	-4.0783e+00
5.7431e+00	7.0460e+00	-2.9337e-01	-2.1276e+01	-1.3857e+02

bcgf =

5.2502e+00	6.4618e-01
-3.2830e-01	2.9101e+00
2.5970e+01	7.3091e+00
1.5589e+01	-7.1255e+00
-1.9609e+01	-4.1407e+00
2.1893e-01	5.2816e+00
5.5783e-01	5.8452e+00
-1.4366e+00	4.0563e+00
-1.2310e+01	2.5979e-01
-2.3522e+00	-5.2653e-02
3.4165e-01	-9.6027e-01
-2.7670e-01	5.1899e-01
-2.0646e-01	-3.9167e-02
6.0765e-02	-1.2386e-01
-5.2177e-03	-5.8883e-03
-5.7008e-02	-1.3306e-02
3.0829e-01	7.1960e-02
-5.1296e-01	-1.1973e-01
1.6850e-01	3.9331e-02
-2.2395e-01	-5.2274e-02
2.5935e-01	6.0536e-02
-1.8438e-01	-4.3038e-02
-8.1148e-02	-1.8941e-02
8.4666e-02	1.9762e-02
-1.0273e-01	-2.3978e-02
-3.0092e-02	-7.0239e-03
3.1136e-03	7.2677e-04
8.3068e-03	1.9389e-03
1.4001e-03	3.2679e-04

ccgf =

Columns 1 through 6

0	0	0	0	0	0	0
0	0	0	0	0	0	0

Columns 7 through 12

0	0	0	0	0	0	0
0	0	0	0	0	0	0

Columns 13 through 18

0	0	0	-6.4236e-01	1.1544e-01	6.0999e-02
0	0	0	-8.3474e-02	-1.3417e+00	-1.5794e+00

Columns 19 through 24

1.4464e-01	3.5829e-01	3.4970e-02	-2.1996e-02	7.9072e-02	-2.7843e-02
-6.1148e-01	4.3076e-01	-6.6611e-01	5.3449e-01	-2.9948e-01	2.2334e-01

Columns 25 through 29

-1.1672e-01	4.0736e-02	3.0755e-02	-3.1054e-02	-1.7417e-03
-2.3373e-01	-7.6955e-02	2.3094e-02	-1.1998e-02	3.0561e-03

dcgf =

0	0
0	0

## APPENDIX E

### Poles of The 3 I/O Reduced Order Closed Loop System

-9.1468e+03  
-5.5159e+02 + 5.3384e+02i  
-5.5159e+02 - 5.3384e+02i  
-2.2777e+02 + 2.3189e+02i  
-2.2777e+02 - 2.3189e+02i  
-1.4457e+02  
-1.4319e+02  
-1.1949e+02  
-8.9079e+01 + 1.8937e+01i  
-8.9079e+01 - 1.8937e+01i  
-1.7935e+01 + 6.0318e+01i  
-1.7935e+01 - 6.0318e+01i  
-5.2531e+01 + 4.8268e+01i  
-5.2531e+01 - 4.8268e+01i  
-4.9021e+01 + 4.9207e+01i  
-4.9021e+01 - 4.9207e+01i  
-3.1654e+01 + 9.6963e+00i  
-3.1654e+01 - 9.6963e+00i  
-2.9006e+01  
-2.0127e+01  
-8.7118e+00 + 9.5608e+00i  
-8.7118e+00 - 9.5608e+00i  
-8.0945e+00 + 6.1691e+00i  
-8.0945e+00 - 6.1691e+00i  
-1.4512e+01  
-1.8891e+00  
-1.9503e+00  
-1.0702e+01  
-2.7168e+00  
-8.6993e+00

## REFERENCES

1. Doyle, J. C. and Stein, G., Multivariable Feedback Design: Concepts for a Classical/Modern Synthesis, IEEE Transactions on Automatic Control, Vol. AC-26, No. 1, pp. 4-16, February 1981.
2. Safonov, M. G., Laub, A. J., Hartman, G. L., Feedback Properties of Multivariable Systems: The Role and Use of The Return Difference Matrix, IEEE Transactions on Automatic Control, Vol. AC-26, No. 1, pp. 47-65, February 1981.
3. Lehtomaki, N. A., Practical Robustness Measures in Multivariable Control System Analysis, Ph.D. Dissertation, Massachusetts Institute of Technology, Cambridge, Massachusetts, May 1981.
4. Gordon, N. C., Utilization of Numerical Optimization Techniques in the Design of Robust Multi-Input Multi-Output Control Systems, Ph.D. Dissertation, Naval Postgraduate School, Monterey, California, September 1984.
5. Chiang, R. Y., and Safonov, M. G., Robust-Control Toolbox, User's Guide, pp. R4-R33, RR9, RR10-RR11, RR26-RR30, The Mathworks, Inc., June 1988.
6. Postlethwaite, I., and others, H<sub>∞</sub> Control System Design: A Critical Assessment, International Federation on Automatic Control, Vol. 8, pp. 328-333, 1987.
7. Kwaakernaak, H., and Sivan, R., Linear optimal Control Systems, John Wiley and Sons, Inc., 1972.
8. Ogata, K., Modern Control Engineering, Prentice-Hall, Inc., 1970.
9. Safonov, M. G., and Chiang, R. Y., CACSD Using the State Space L<sub>∞</sub> Theory: A Design Example, IEEE Transactions on Automatic Control, Vol. 33, No. 5, pp. 477-479, May 1988.
10. Jane's All the World's Aircraft 1987-1988, Jane's Information Group Limited, 1988.
11. V. C. Gordon and D. J. Collins, Multi-Input Multi-Output Automatic Design Synthesis for Performance and Robustness, AIAA Journal of Guidance, Control, and Dynamics, Vol. 9, No. 3, pp. 281-287, May-June 1986.
12. Hidenori Kimura, Robust Stabilizability for A Class of Transfer Functions, IEEE Trans. Automat. Contr., VOL. AC-29, No. 9, pp. 788-793, Sept. 1984.

13. W. L. Rogers, Applications of Modern Control Theory Synthesis to A Super-Augmented Aircraft, M.S. Thesis, Naval Postgraduate School, Monterey, California, June 1989.
14. Bernard Friedland, Control System Design: An Introduction to State Space Methods, McGraw-Hill Book Company, 1986.
15. Bruce A. Francis and others, H<sub>∞</sub> - Optimal Feedback Controllers for Linear Multivariable Systems, IEEE Trans. Automat. Contr., vol. AC-29, No. 10, pp. 888-899, Oct. 1984.

## INITIAL DISTRIBUTION LIST

	No. copies
1. Defense Technical Information Center Cameron Station Alexandria, VA 22304-6145	2
2. Library, Code 0142 Naval Postgraduate School Monterey, California 93943-5000	2
3. Chairman, Code 69Hy Department of Mechanical Engineering Naval Postgraduate School Monterey, California 93943-5000	2
4. Professor D. J. Collins, Code 67Co Naval Postgraduate School Monterey, California 93943-5000	5
5. Professor Liang-Wey Chang, Code 69Ck Naval Postgraduate School Monterey, California 93943-5000	1
6. Main Library P. O. Box 8243, Ta-Hsi, Tao-Yuan, 33500 Taiwan, Rep. of China	1
7. Mr. Ta-Chieh Hsu P. O. Box 8243-23, Ta-Hsi, Tao-Yuan, 33500 Taiwan, Rep. of China	3
8. Mr. Tor W. Jensen Code 6013 Naval Air Development Center Warminster, Pennsylvania 18974	1
9. Mr. Joe Gera NASA Dryden Flight Research Center P.O. Box 273 Mail Code OFDC Edwards, California 93523	1

10. Mr. Thomas Momiyama 1  
AIR 931  
Naval Air Systems Command  
Washington, D.C. 20361-0001
  
11. Mr. George Derderian 1  
AIR 931E  
Naval Air Systems Command  
Washington, D.C. 20361-0001